Ministère de l'Enseignement Supérieur et de la Recherche Scientifique
Université Mohammed Boudiaf à M'sila
Faculté de Technologie
Département d'Électronique

Mémoire de Master

Domaine : Télécommunications

Spécialité : Ingénièrie des Télécommunications

Thème :

A performance analysis of NOMA, RIS, and RIS-aided NOMA

(*Une analyse des performances de NOMA, des RISs et de NOMA assisté par des RISs*)

Présenté par :
- ACHOURI Mohammed
- BENKIHOUL Abdelhafid

Sujet proposé et dirigé par :
- Dr. BENMAHMOUD Slimane

Devant le jury composé de :

Dr. GARAH Messaoud	Président
Dr. BENMAHMOUD Slimane	Encadreur
Prof. BENMEDDOUR Fadila	Examinateur

Projet N : ..../2023

Dedications

For the sake of God our creator and lord. To our teacher and great messenger Muhammad (peace and blessings of Allah be upon him) who taught us the purpose of life.

To our fathers and mothers for their endless love, support and encouragement . To our beloved brothers and sisters . To our colleagues and teachers in the faculty of technology at MOHAMED BOUDIAF university –M'SILA.

M. A & A. B

Acknowledgments

First of all, I am deeply grateful to The Almighty Allah (SWT), the Most High, the Most Compassionate, and the Most Merciful for all his giving and for the opportunity He gave me to study, to research and to write and finalizing this thesis . I Thank Allah, my outmost thanks, for providing me this opportunity and granting me the capability to proceed successfully.

I must acknowledge my advisor Professor SLIMANE BENMAHMOUD , the person to whom I wish to convey my solidest gratitude and profound respect and to whom I am indebted to for this whole thesis work. It was a great experience to work with him. He acquainted me with the world of advanced research. His mentorship has been tremendously helpful, and his vision and insight never cease to surprise me. His friendly guidance, suggestions and wholehearted supervision has made it possible for me to complete this thesis. I am grateful to him for his useful directions, continuous encouragement, consistent support and valuable remarks throughout the progress of this work. My completion of this work could not have been accomplished without his deepest expertise and the shrewder insight. I have really learned a lot from his comments and suggestions.

Finally, I would like to take this opportunity to thank all my friends and colleagues and the staff at the Department of Electronics, at MOHAMED BOUDIAF university - M'SILA who have given their support and helped me in completing this work.

M. A

Contents

Table des figures

Introduction

The advent of mobile communication technology has had a profound impact on wireless networks, leading to a remarkable increase in the number of mobile networks. This has enabled the society to experience greater connectivity and mobility, accompanied by substantial growth in traffic volume, diverse network usage patterns, higher data consumption rates, and various other scenarios. Consequently, network traffic is expected to witness significant expansion. Presently, mobile devices have become the most prevalent personal gadgets, and the popularity of other devices like wearable and smart devices is also on the rise. To cater to the evolving demands that previous generations of systems were unable to address, the deployment of 5G cellular communication systems is crucial and should be widely implemented.

Despite the advancements made in 4G wireless network technology, meeting the demands of wireless network services that necessitate high speed, rapid response, high consumption, and energy efficiency remains challenging. Consequently, these features have become critical requirements for future 5G services. Presently, 4G/LTE networks are unable to provide instant cloud services, interactive Internet capabilities, enhanced vehicle-to-everything (eV2X) communication, Internet of Things (IoT) connectivity, and seamless communication with drones and robotics while maintaining a superior user experience. As a result, there have been significant global advancements in the field of transmission technology.

This transformative wave of technological advancements is reshaping our lives, work dynamics, and interactions. It has brought forth remarkable services and applications, including self-driving cars, artificial intelligence, smart homes, smart factories, smart cities, and drone-based delivery systems. The future of wireless settings will witness further expansion through the establishment of a symbiotic relationship between devices and human-guided interactions.

The capabilities of mobile phone communication will continue to expand, permeating all aspects of public life and creating a multidimensional ecosystem centered around consumers. Hence, addressing cost-effectiveness becomes crucial. With the expected surge in traffic volume and extensive connectivity growth, numerous implications are on the horizon. Mobile networks will need to deliver a thousand times the spectral efficiency compared to current technology frameworks to accommodate this significant traffic increase. It is worth noting that 4G networks have already demonstrated an increase in spectrum efficiency (SE).

The 5G network integrates several cutting-edge technologies, including the Internet of Things (IoT), device-to-device (D2D) communications, software-defined networking (SDN), mobile edge computing (MEC), cloud computing, and cloud radio access networks (CRANs).

Non-orthogonal multiple access (NOMA) has emerged as a promising technology in the field of wireless networks, offering improved spectral efficiency and enhanced connectivity. Unlike traditional orthogonal schemes such as orthogonal frequency-division multiple access (OFDMA) used in 3GPP-LTE and 5G New Radio Phase 1 standards, NOMA allows multiple users to transmit simultaneously on the same frequency and time resource by combining their signals in the power domain. To successfully decode these combined signals at the receiver, successive interference cancellation (SIC) techniques are utilized.

This thesis investigates the fusion of reconfigurable intelligent surfaces (RISs) with non-orthogonal multiple access (NOMA), utilizing the unique properties of metamaterials and large arrays of cost-effective antennas. The aim is to actualize the concept of intelligent radio environments by harnessing the capabilities of RISs alongside NOMA.

Content and organization of this thesis :

This thesis is organized into five chapters. In **the first chapter** we give an overview of wireless communications.

In **the second chapter**, we deal with orthogonal and non-orthogonal multiple access (OMA/NOMA) techniques and the key technologies enabling their applications.

In **the third chapter**, the secrets of IRS-assisted communications systems are revealed.

The fourth chapter deals with hybrid NOMA/OMA networks assisted by IRSs in their downlink and uplink versions.

In **the last chapter**, we present the simulation results of the performance of NOMA and IRSs-NOMA networks.

Finally, the conclusion summarizes our work and presents new research perspectives in the field of IRSs and NOMA.

1 An overview of wireless communications

In this chapter,we'll first go through a brief history on wireless communications. Then, we'll explain what exactly communication is and what's the benefit to be wireless. We'll also talk about current trends in mobile networks and finally give an overview of its 5G version.

1.1 A brief history of wireless communications

Wireless communication technology plays a crucial role in various aspects of our daily lives. It is an integral component of essential devices such as telephones, radios, the Internet, and smartphones. All of these rely on some form of wireless technology for their functionality [3]. One of the earliest methods of wireless transmission can be traced back to ancient China, where smoke signals were employed as a means of communication. Guardians stationed along the Great Wall would ignite smoke signals to notify nearby towers of impending attacks. Smoke signals had the remarkable ability to be visible from a distance of approximately 300 miles, enabling towers to receive timely alerts [4]. In 1880, Alexander Graham Bell invented and obtained a patent for his telephone. Together with his assistant Charles Sumner Tainter, they achieved a significant milestone by transmitting the first wireless telephone message using the photo phone. Unlike traditional telephones that relied on electricity, the photo phone transmitted sound through light [5]. In 1873, James Clerk Maxwell formulated the theory of electromagnetism, laying the foundation for our understanding of the relationship between electricity and magnetism. Building upon Maxwell's theory, Heinrich Hertz conducted experiments in 1886 that provided empirical evidence for the existence of radio

waves. Hertz's discoveries marked a significant milestone in the field of wireless communication [6]. The exact inventor of the radio is a topic of debate, but in 1891, Nikola Tesla successfully showcased a functional wireless radio during a lecture. Tesla's demonstration played a significant role in the development of radio technology[3]. In 1897, Guglielmo Marconi obtained a patent for his wireless telegraph, which he had developed. By 1901, people started exploring various aspects of radio technology. Broadcasting stations were established, and on November 2nd, 1920, Pittsburgh's KDKA station made the first-ever commercial broadcast. This significant event occurred on election day, allowing people to hear the presidential race results before reading about them in newspapers. In 1922, the British Broadcasting Company made its inaugural public broadcast from a London studio owned by Marconi. In the same year, The Toronto Star initiated its own radio station and became the first station to broadcast a hockey game a year later, featuring Foster Hewitt. However, radio encountered challenges such as poor audio quality caused by static and interference from sky waves. The issues with radio interference were addressed in 1933 with the development of Frequency Modulation (FM) by Edwin Armstrong. FM technology offered improved sound quality compared to Amplitude Modulation (AM). Initially, radio stations operated within the 42 to 50 megahertz band, but eventually shifted to the higher frequency range of 88 to 108 megahertz [7]. The numerous advancements in wireless transmission have made it an integral part of the Information Age we live in today. Satellites, intentionally launched into Earth's orbit, are among the commonly used objects that play a significant role in facilitating various services such as television, radio, internet, and navigation systems like the Global Positioning System (GPS). Other wireless technologies include WiFi, enabling wireless internet access on mobile devices without the need for Ethernet or USB cables; Bluetooth, which facilitates wireless connections between devices; and Infrared, which transmits information wirelessly through infrared radiation [4]. The primary advantage often associated with wireless transmission is its ability to provide mobility, allowing users to stay connected and access information on the go. However, a notable drawback is the potential for interference between wireless connections, which can affect the quality and reliability of the transmission [3]. It is evident that our reliance on wireless transmission has become increasingly significant in today's technological landscape.

1.2 What exactly communication is and what's the benefit to be wireless ?

Communication is the fundamental process of exchanging information. It can be classified into two main categories : wired communication and wireless communication. Wired communication utilizes cables as the medium to transmit information from a source to a destination [3]. Wired Communication offers the potential to handle numerous tasks. However, there are challenges associated with its infrastructure setup and cable installation, which can be both costly and time-consuming to address. In remote areas, the establishment of Wired Communication can be particularly challenging [5], [3]. So in order to overcome the problems encountered by Wired Communication, Wireless Communication has been used. The introduction of Wireless Communication has brought about increased mobility and global connectivity. This form of communication enables the transfer of information from a source to a destination without the need for any physical medium [4]. Wireless Communication eliminates the possibility of communication failure, unlike in Wired Communication where cables can be susceptible to damage from environmental conditions. In scenarios such as floods or other disasters, Wireless Communication incurs minimal loss to the communication infrastructure compared to Wired Communication [5]. The figure below shows the block diagram of a wireless communication system.

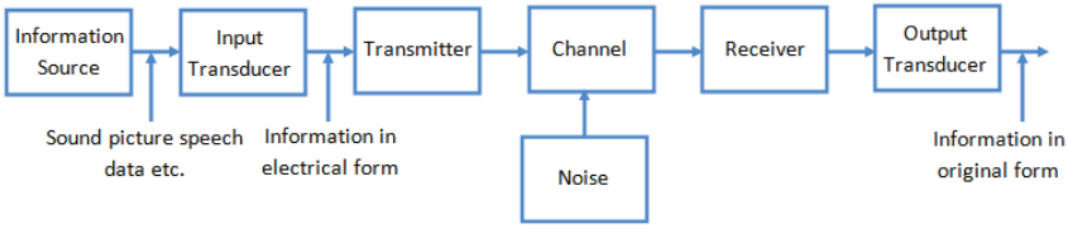

FIGURE 1.1 – A block diagram for a generic wireless communication system.

The initial component in the communication system is the source, which generates the message signal. This message signal can take the form of non-electric data, which is then converted into an electrical signal using a transducer. For instance, a microphone converts our voice into an electrical signal. The next component is the transmitter, responsible for various signal processing tasks such as restricting the range of audio frequencies, signal amplification, and modulation.

The channel represents the medium through which the message travels from the transmitter to the receiver. However, unwanted signals, known as noise, can interfere with the desired signal during transmission. The receiver block is responsible for reproducing the message signal in its electrical form. Finally, the output transducer block serves as the last stage, converting the received electrical message signal back into its original form.

1.3 Current Trends in Mobile Networks

The growth of mobile subscribers may lead to the explosively increasing mobile data traffic. The latest data from [8] indicates that the global mobile broadband subscriptions have reached the 5.1 billion figures in 2018 and it is predicted to grow to 5.7 billion by 2023. Furthermore, the number of connected devices may surpass the global population in the future due to the growth of machine-to-machine (M2M) communications and Internet of Things (IoT) applications, which further contributes to global mobile traffic growth. In addition, the demand for rich multimedia content has increased drastically in recent years and hence inevitably contributes to further increase in mobile traffic.

As highlighted by a study in [9], mobile video content contributed more than half of the global data traffic since 2012 and it is expected to reach 78% of global traffic by 2021, prompting the need for thousand-fold increase in capacity and wireless resources in order to accommodate the mobile traffic demand. Innovative solutions, including massive MIMO, network densification and advanced multiple access schemes, are crucial to address the challenges of the ever-increasing capacity requirement [10].

There are high expectations for the fifth generation (5G) technology to effectively support advanced and crucial applications, which have been broadly categorized by the International Telecommunication Union (ITU) into three main groups : enhanced mobile broadband (eMBB), massive machine-type communication (mMTC), and ultra-reliable and low-latency communication (URLLC). To meet the demands of these use cases, the ITU has outlined specific performance

targets. These targets encompass peak rates of 20 Gbps for downlink and 10 Gbps for uplink, a user experience data rate of 100 Mbps, latency below 1 ms, mobility support up to 500 km/h, and connectivity density reaching 1 million devices per square kilometer, as detailed in [11].

1.4 An Overview of the 5G Mobile Networks

Wireless communications have emerged as an essential technology in contemporary society, progressing from the initial generation (1G) to 5G. Being the most recent iteration in wireless network technology, 5G networks have been designed to address the exponential surge in demand for data traffic due to the rise and expansion of the internet of things (IoT) and innovative applications like tactile internet, high-definition video streaming, telemedicine, remote surgery, intelligent transportation, and instantaneous control [12], [13].

Considering diverse user requirements, the International Telecommunication Union (ITU) has classified 5G networks into three distinct generic service scenarios : enhanced mobile broadband (eMBB), massive machine-type communications (mMTC), and ultra-reliable low-latency communications (URLLC) [14]. These three scenarios correspond to three demands, which arepeak data rate, connectivity density, and latency, respectively. Note that notall demands need to be fulfilled simultaneously [13].

2

Multiple access techniques : Orthogonal and non-orthogonal (OMA/NOMA)

In this chapter,we'll first go through an overview of multiple access techniques. After that, we'll talk about NOMA, the key technologies enabling it, and its system model in its bot downlink and uplink scenarios. Finally we'll compare NOMA and OMA.

2.1 An overview of Multiple Access Techniques

In network access, multiple users utilize multiplexing, a technique that involves merging several signals and transmitting them through a shared channel. This method allows for efficient utilization of the channel's capacity, enabling multiple users to transmit their signals simultaneously without causing significant interference or congestion. Multiplexing plays a crucial role in optimizing communication systems by allowing multiple data streams to coexist and be transmitted through a single channel, thereby enhancing overall network efficiency and data transmission rates [15]. When the technique of multiplexing is employed to enable multiple users to engage in communication over a shared channel, it is referred to as multiple access. Essentially, multiple access is the practical implementation of multiplexing in communication systems. An illustration of this concept is seen in the scenario of a WiFi hotspot that distributes its internet connection among various users. Each user is allocated a specific frequency block within which they can transmit and receive data, exemplifying the principles of multiple access [16]. The larger the size of the block, the higher the throughput achieved.

Multiple access can be categorized into two main types : Orthogonal Multiple Access (OMA) and Non-Orthogonal Multiple Access (NOMA). NOMA operates by utilizing the power domain or code domain to enable efficient communication among users [15]. There exist four main OMA techniques, namely

- Frequency division multiple-access (FDMA)
- Time division multiple-access (TDMA)
- Code division multiple-access (CDMA)
- Orthogonal frequency division multiple-access(OFDMA)

2.1.1 Frequency division multiple-access

In Frequency division multiple-access the frequency spectrum is divided into different slots. Each time slot is assigned to a device within the wireless network. We've observed a variety of devices functioning within different ranges, including the wireless personal area network, wireless metropolitan area network, and wide area network. Additionally, protocols such as ZigBee, Bluetooth, and WiMAX contribute to this diversity. Each device is allocated a distinct frequency based on the designated division. To prevent interference, it's important to leave certain frequencies and bands unallocated [15], [17] .

2.1.2 Time division multiple-access

To address the challenges stemming from the non-allocation of certain bands, a solution involves arranging devices into distinct time slots [18]. When allocating time t1 to Device 1, it can exclusively engage in data transfers or other tasks within that specific time frame. The frequency spectrum is designated for a brief interval, referred to as a Time Frame (TF). Each assignment requires waiting for a new TF [19].

2.1.3 Code division multiple-access

To address the challenges posed by TDMA, a solution known as Code Division Multiple Access (CDMA) has emerged. CDMA employs a unique coding scheme for transmitting signals, thus eliminating interference concerns. This approach allows all devices to utilize the available frequency for data transmission simultaneously. However, CDMA assumes that all devices receive signals at the same power level. The issue of varying power levels is managed through power control techniques [20].

2.1.4 Orthogonal frequency division multiple-access

Orthogonal Frequency Division Multiple Access (OFDMA) employs a distinct frequency allocation approach where data is transmitted in a manner akin to being at right angles. This enables multiple users, potentially an unlimited number, to simultaneously utilize the data without encountering interference or signal jamming. This technique is essentially an extension of the multi-user OFDMA scheme, incorporating a multiplexing approach that operates on orthogonal frequency divisions. The technique assigns specific subsets of carriers to individual users, facilitating effective implementation of this multiple-access strategy. Each user is allocated a specific time interval during which they can engage in a multitude of activities. This ensures that user 1 utilizes their allotted time for data transmission or any other operations, followed by user 2 utilizing their designated time slot. This approach guarantees an absence of interference or signal overlap, resulting in efficient data transfer. In comparison to other methods, this technique enables seamless data transmission and is particularly effective in supporting simultaneous, low-power data transfer. The primary benefit lies in the occurrence of activities that overlap in a perpendicular manner. It's noticeable that each user is assigned at a distinct right angle, ensuring a division that aligns with these angles [21], [15].

2.2 Non-Orthogonal Multiple Access (NOMA)

NOMA allows multiple users to be allocated in the same frequency and timere sources by exploiting another domain such as power or code, producing intentional non-orthogonality for signals among the users and thus allowing mutual interference among the users. NOMA can be further classified into two major categories ; power domain and code domain NOMA [22], [23].

Code-domain NOMA includes various multiple access schemes like sparse code multiple access (SCMA), low-density spreading CDMA (LDS-CDMA), and multiuser shared access (MUSA). Power domain NOMA improves the spectral efficiency by multiplexing the users' signals in power domain using superposition coding (SC) at the transmitter and applying successive interference cancellation (SIC) at the receiver to detect the users' signals. In addition, power domain NOMA can achieve robust performance gain regardless of channel state information (CSI) feedback latency and UE mobility [24], [25]. Transmitters rely on receiver CSI knowledge for tasks like transmit power allocation and user pairing. Simultaneously, receivers require CSI information for user demultiplexing [26].

2.3 The Key Technologies Enabling NOMA

The fundamental idea of NOMA is to exploit the power domain as a new dimension to achieve multiplexing. To enable the application of NOMA, two main techniques, namely Superposition Coding (SC) and Successive Interference Cancellation (Successive Interference Cancellation (SIC)) , are introduced. In particular, SC must communicate two messages simultaneously by encoding them into one message unique in two layers, and SIC must decode the desired message from the superimposed message. With the development and maturity of these two techniques, NOMA can be applied regardless of the difficulty of implementation [27].

2.3.1 Superposition coding

In NOMA, the signals of multiple users are superposed in power domain using Superposition coding (SC) at the transmitters. SC is a non-orthogonal approach which combine user's information into a single signal source and hence able to achieve the capacity on a scalar Gaussian broadcast channel [28]. This allows multiple users'information to be transmitted at the same frequency and time resources.

2.3.2 Successive Interference Cancellation

Successive interference cancellation (SIC) is a well-known physical layer technique [29]. Briefly, SIC is the ability of a receiver to receive two or more signals concurrently (that otherwise cause collision in current wireless networks based on IEEE 802.11 standard). SIC is possible because the receiver may be able to decode the stronger signal, subtract it from the combined signal, and extract the weaker one from the residue. Emerging software radio platforms, such as GNU radios, are making practical implementations of SIC feasible [30], [31]. A natural question then is : given SIC capable radios, what are the implications on MAC protocol design ? Can SIC be exploited at the MAC layer to improve throughput ? What is the scope and what are the limitations ? Inspired by these questions, this paper is an attempt to interpret the PHY layer SIC capabilities from the MAC layer. We limit our focus to the special case of SIC, where only one signal is cancelled from another. We consider simple topological configurations that form the building blocks of larger networks, and systematically study the ideal gains available from SIC. Even among the simple building blocks, we recognize that certain topological patterns are amenable to SIC gains, while others are not. In an attempt to tap into some of these gains, we find that link layer coordination, such as SIC-aware link pairing and power control, are necessary. We verify these observations through theoretical formulations. Guided by these outcomes, we carve out the scenarios in which SIC-aware protocols are worth pursuing. We develop an algorithm for such scenarios, and evaluate its performance [32].

2.4 NOMA's System Model

NOMA disrupts orthogonality by assigning the same time/frequency resource to multiple users, albeit with added complexity at the receiver end. On the transmitting end, distinct power levels are assigned to signals from various users (thus the term "power domain"), and superposition coding is utilized to send out the combined signals of the users. In the following subsections, we delve into the system model of NOMA, including signal superposition and SIC, in both downlink and uplink scenarios.

2.4.1 Downlink NOMA transmission

Let x_1 and x_2 be the multiplexed signals of UEs 1 and 2, with respective powers p_1 and p_2, and let h_1 and h_2 be their experienced channel gains with $|h_1| > |h_2|$. In the NOMA framework, UE2 is referred to as the strong user, while UE1 is labeled as the weak user. A higher power level is allocated to the weak user ($p_1 > p_2$) to compensate for its weaker channel gain, provide user fairness, and allow the decoding of UE1's signal at the level of UE2. The super-imposed signal transmitted by the Base Station (BS) is given by

$$x = \sqrt{p_1}x_1 + \sqrt{p_2}x_2, \tag{2.1}$$

and the received signals y_1 and y_2 at the level of UE 1 and UE 2 are given respectively by

$$y_1 = h_1 x + n_1, \tag{2.2}$$

and

$$y_2 = h_2 x + n_2, \tag{2.3}$$

where n_i represents the Gaussian noise received by UE i with average power σ^2.

As shown in Fig. 2.1, at the level of UE 2, the SIC receiver is applied to extract x_2 from the total received signal. It proceeds first by detecting, demodulating and decoding the dominant signal which is x_1, prior to subtracting it from the total received signal.

Consequently, x_2 is decoded in an interference-free manner and its achievable rate according to the Shannon channel capacity theorem is given by

$$R_2 = \log_2\left(1 + \frac{P_2\,|h_2|^2}{\sigma^2}\right), \tag{2.4}$$

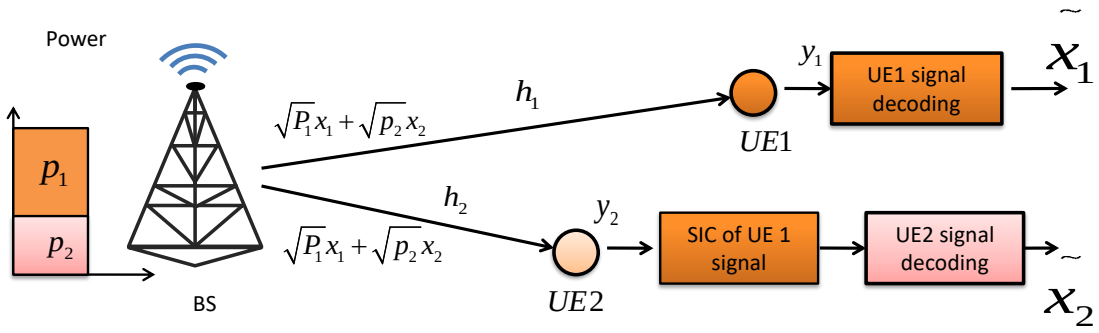

FIGURE 2.1 – Two users NOMA transmission in the downlink where UE2 performs SIC before retrieving its own signal.

At the level of the weak user, UE2'signal is treated as additional interference, and the achievable rate is given by

$$R_1 = \log_2\left(1 + \frac{P_1 |h_1|^2}{P_2 |h_1|^2 + \sigma^2}\right), \tag{2.5}$$

For the general case of m multiplexed users with channel gains such $|h_1| > |h_2| > ... > |h_m|$, the power is allocated according to the descending order of channel gains. The ith UE iteratively decodes and subtracts the signals of users with weaker channel gains before retrieving its own signal x_i while suffering from the interference of the remaining $i-1$ users. The rate for UEi is thus given by

$$R_i = \log_2\left(1 + \frac{P_i |h_i|^2}{\sum_{j=1}^{i-1} P_j |h_i|^2 + \sigma^2}\right). \tag{2.6}$$

2.4.2 Uplink NOMA transmission

We consider two users transmitting respectively signals x_1 and x_2 to the base station (BS). The power of signals x_1 and x_2 arep_1 and p_2, respectively (Fig. 2.2). The received signal at the BS is hence a superposition of x_1 and x_2

$$y = h_1\sqrt{p_1}x_1 + h_2\sqrt{p_2}x_2 + n. \tag{2.7}$$

In this case, x_1 is decoded first by considering x_2 as noise. Its signal-to-interference-plus-noise ratio is

$$SINR_1 = \frac{g_1 p_1}{\sigma^2 + g_2 p_2} \tag{2.8}$$

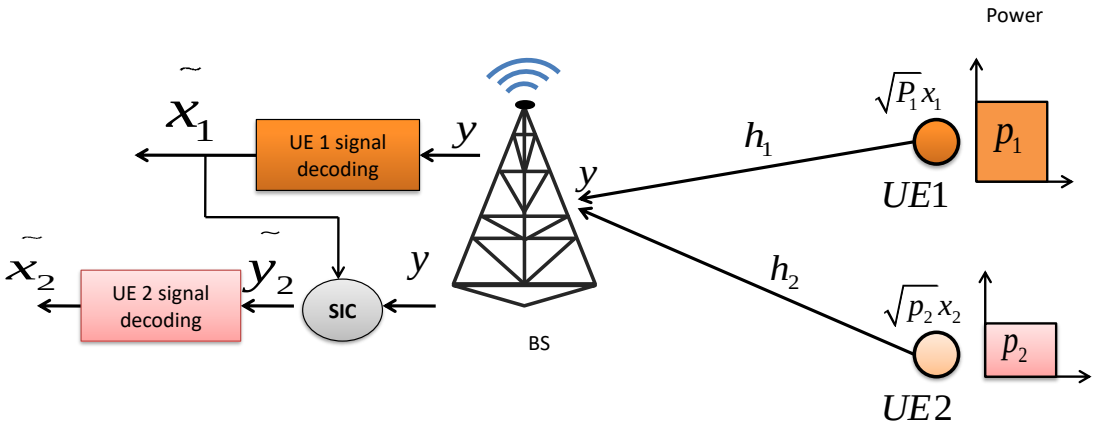

FIGURE 2.2 – Two users NOMA transmission in the uplink.

where $g_1 = |h_1|^2$ and $g_2 = |h_2|^2$ are the channel gains. Assuming that user 1's signal as been correctly decoded, $\tilde{x}_1$ is then subtracted from the superposed signal y (see block SIC in Fig. 2.2) to get signal $\tilde{y}_2 \approx h_2\sqrt{p_2}x_2 + n$ in which the interference caused by user 1 is canceled out. This is the principle of successive interference cancellation (SIC) : when multiple signals are superposed, the first decoded signals are subtracted from y before decoding the next signal. The signal-to-interference-plus-noise ratio of x_2 after SIC is :

$$SINR_2 = \frac{g_2 p_2}{\sigma^2} \tag{2.9}$$

In this case, the NOMA data rates are :

$$R_1' = \log_2\left(1 + \frac{g_1 p_1}{\sigma^2 + g_2 p_2}\right) \tag{2.10}$$

$$R_2' = \log_2\left(1 + \frac{g_2 p_2}{\sigma^2}\right) \tag{2.11}$$

2.5 NOMA vs OMA

In terms of the spectral efficiency and the users' fairness, we can say that

1. In OMA, such as in the case of OFDMA, a specific frequency resource is assigned to each user regardless of their individual channel conditions [33]. Consequently, this resource allocation approach leads to lower spectral efficiency. Furthermore, the allocation is based on channel conditions, prioritizing users with better channel conditions over those with poorer conditions [33], [34], [35], [36]. Consequently, users with worse channel conditions have to wait for resource allocation, resulting in fairness concerns.

2. NOMA, on the contrary, provides the capability to allocate resources to multiple users without considering their channel conditions, resulting in improved user fairness [37], [38]. In NOMA, users are assigned the same frequency resource, regardless of their channel conditions, allowing both weak and strong users to utilize the resource simultaneously. As a result, the spectral efficiency in a NOMA system exhibits a significant improvement compared to an OMA system [39], [40], [41].

3

Intelligent reflecting surfaces (IRS)-aided Wireless communications

In this chapter, we'll go trough an introduction to IRS-aided Wireless communications. Then, we'll see some of its applications. After that, we'll be presenting the challenges facing their applications. Finally, we'll make a literature review on IRSs.

3.1 Introduction to IRS-aided Wireless communications

Recent advancements in electromagnetic materials have revealed the potential to transform the wireless channel using an innovative type of affordable material known as meta-material, which has been explored extensively [42], [43]. The engineered thin layer composed of this material is commonly denoted as a reconfigurable intelligent surface (RIS), intelligent reflecting surface (IRS), or meta-surface [44], [45], [46]. For wireless communication, it is often used in the literature to use IRS8 and RIS.

3.1.1 The Structure of an IRS element

An IRS can consist of a relatively straightforward 2D configuration, composed of conductive patches, diodes, and conductive power/signal lines. This structure includes a positive-intrinsic-negative (PIN) diode, and the associated biasing circuitry is depicted in Fig. 3.1.

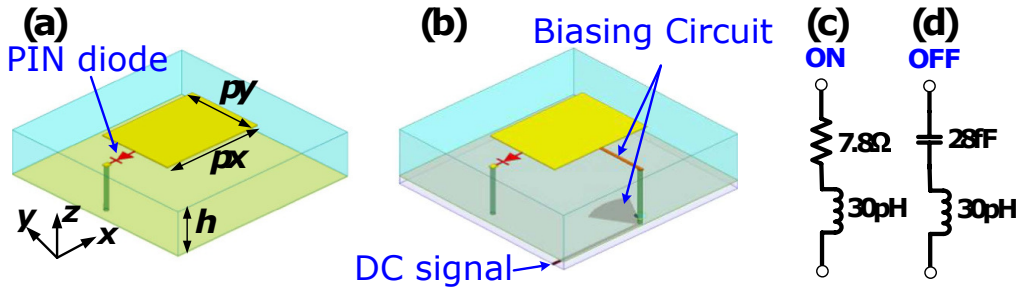

FIGURE 3.1 – The structure of an IRS unit (As proposed in [1]). (a) Schematic of the element, with specific dimensions. (b) The biasing architecture. (c,d) The equivalent circuits of the PIN diode at ON and OFF states, respectively.

A diagram illustrating the structure of an IRS element is shown in Fig. 3.1(a). This unit features a sandwich-like configuration, comprising a basic rectangular patch and a metal ground plane, with a substrate positioned between them that possesses specific dielectric constant and loss tangent values [47]. A PIN diode is utilized to establish a connection between one edge of the patch and the ground using a metal via. This configuration results in an anisotropic element that exhibits binary-coded reflective characteristics along the x direction. To simplify the biasing process in real-world applications, a direct-current (DC) circuit is incorporated into the element's design, as depicted in Fig. 3.1(b). The deliberately designed bias circuit includes the quarter-wavelength microstrip line, the open-ended radial stub and DC signal line. The quarter-wavelength microstrip line and the open-ended radial stub are employed to choke the RF signal and ensure a good isolation between the DC and RF performance. The PIN diode is modeled as an equivalent circuit shown in Fig. 3.1 (c,d) when biasing circuit is switched ON or OFF, respectively.

Furthermore, it is noticeable that numerous elements are compactly arranged within an array-style structure to compose a surface. Through the integration of multiple elements in this array-like meta-material surface, the intelligent reflecting surface (IRS) can achieve a diverse range of manipulative functions on the incident electromagnetic (EM) wave [1]. Particularly, the EM wave that is reflected can be skillfully controlled in terms of its polarization state, power distribution, and concentration towards any chosen direction. In order to achieve such specific functions, precise manipulation of the excitation and phase of individual electronic elements is necessary, which is accomplished through processors utili-

zing a predetermined control strategy, such as employing a field programmable gate array (FPGA) [42], [48]. This approach enables the manipulation of the phase and amplitude of the incoming EM wave on the surface, allowing for controlled reflection in desired directions. This forms the basis for creating a programmable wireless channel.

3.1.2 The architecture of an IRS unit

The architecture of an RIS unit is shown in Fig.3.2, where a thin planar surface of multiple unit cells is connected to a smart controller. The unit cells are the main constructing component of the RIS, whereas the role of the smart controller is to adapt the interaction of the unit cells to the impinging waves. In general, the concept of metamaterial is the key enabler for building the RIS. The research field of metamaterial is interested in building materials of reconfigurable EM properties that don't exist in natural materials [49]. The RIS is commonly referred to

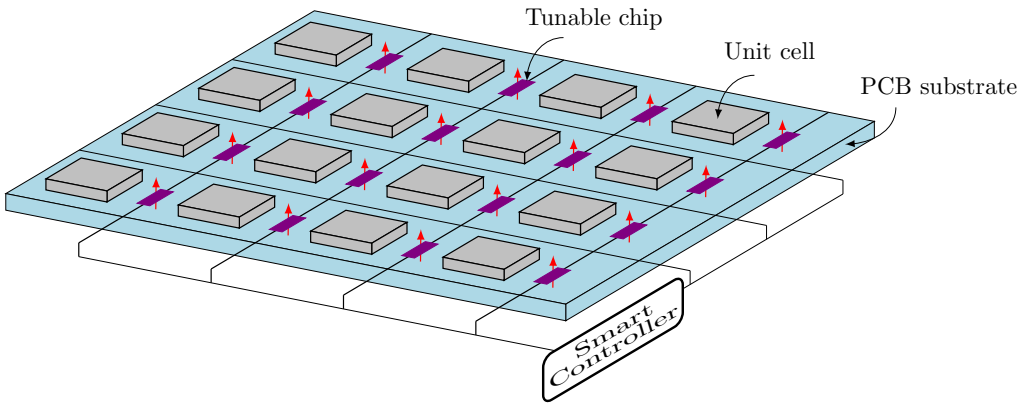

FIGURE 3.2 – The architecture of RIS

as a meta-surface due to its ability to manipulate electromagnetic waves. It is also known by various other names, including intelligent reflecting surface, large intelligent surface, digitally controllable scatterers, and software controllable surface. On the other hand, the individual building block of the RIS, the unit cell, is referred to as a meta-atom, reflecting element, or scattering element. Conceptually, a unit cell can be visualized as a sub-wavelength scattering particle, such as a small antenna, connected to tunable electronic circuits. These circuits, which may involve components like PIN diodes, varactors, or MEMS switches, enable

the configuration of the unit cell's response to incident electromagnetic waves. The ability of the RIS to manipulate electromagnetic waves primarily lies in its control over the reflection coefficient of each unit cell in response to the incoming waves [50].

The alteration of the unit cell's reflection coefficient is commonly achieved by controlling the load impedance connected to the reflecting element [51]. For example, when using a tunable chip like a PIN diode for each element, the PIN diode can be switched between on and off states by adjusting its bias voltage. This variation in the load impedance connected to the element results in a phase shift difference of π for the reflection coefficient between the on and off states. To enable full control over the phase shift, multiple PIN diodes or a varactor can be connected to each unit cell, providing multiple choices or continuous configuration for the connected load impedance. Additionally, the amplitude of the reflection coefficient can be adjusted by incorporating a variable resistor load for each unit cell. This allows control over the portion of incident wave energy dissipated in the unit cell [52].

Furthermore, a significant benefit of the RIS is its exceptional energy efficiency, as it does not require power amplifiers, radio frequency (RF) chains, or complex signal processing capabilities. This characteristic has led to the widespread recognition of the RIS as a nearly passive device since it does not consume power for transmission, with the primary energy being utilized in the control process of the tunable circuits to manipulate the impinging waves. However, it is worth noting that active RISs, which have the ability to amplify the impinging radio waves, can be achieved by integrating amplifiers into the unit cells [53].

3.1.3 The electromagnetic functions of an IRS

The RIS can be configured to support multiple functions for the incident EM waves. In Fig. 3.3, we discuss some of the possible functions of the RIS :

- Reflection : The RIS is configured such that the incident EM wave is reflected towards a specified direction where the angle of reflection doesn't necessarily be equal to the angle of incidence according to the generalized Snell's law [54].

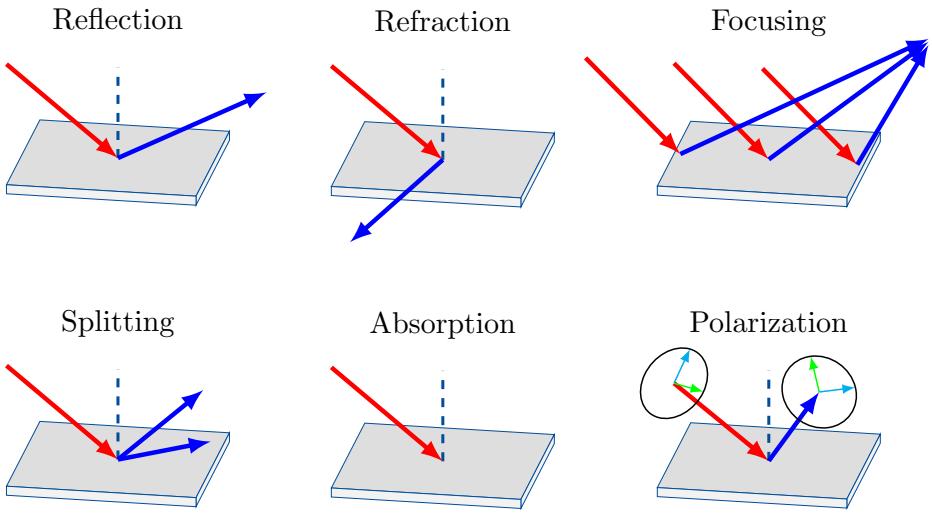

FIGURE 3.3 – The electromagnetic functions of RIS.

- Refraction : The RIS refracts the impinging waves towards a specified direction. However, in this scenario, the RIS is commonly manufactured from unobstructed material towards EM waves such as a glass substrate [55].
- Focusing : The RIS focuses all the scattered waves from the unit cells at a certain location to maximize the received signal strength there. This function can be achieved by adjusting the phase shifts induced from all the unit cells in the RIS such that the scattered paths are added constructively at a certain location.
- Splitting : The RIS creates multiple reflected and refracted waves for a single impinging wave. This function can be satisfied by dividing the RIS into several sub-surfaces and configuring them independently to split the incident wave.
- Absorption : The RIS ensures minimum reflection and refraction power of the impinging waves which may be possible by controlling the amplitude reflection coefficients of the unit cells [56].

- Polarization : The RIS is utilized to change the polarization state between the incident and reflected/refracted waves [1]. This function usually relies on dual-polarized unit cells which could excite two orthogonal polarization states and induce independent phase shifts per each polarization state whenever a wave is incident on them.

3.1.4 A Practical model for the IRS unit

The majority of current research on RIS-aided wireless communications assumes an ideal reflection model for the unit cells, where the amplitude and phase of the reflection coefficient are treated as independent variables. Therefore, in existing literature, it is commonly assumed that the unit cells have a unity amplitude reflection coefficient regardless of the phase shift. However, achieving this assumption in practice is challenging due to hardware limitations. The actual reflection coefficient of the unit cells is significantly influenced by factors such as resonance frequency, loss resistance, quality factor, and the frequency of the impinging wave. Recent studies, such as [57] and [58], have demonstrated that a practical RIS exhibits a fundamental relationship between the amplitude and phase of the reflection coefficient. These findings highlight the need to consider the interdependency between the amplitude and phase in practical RIS designs, deviating from the idealized assumptions commonly made in previous research.

An RIS is commonly manufactured using a similar process to a printed circuit board (PCB), as depicted in Fig. 3.2. The unit cell structure typically consists of a metallic patch positioned on the upper layer of the dielectric PCB substrate, along with a metal sheet on the lower layer [59]. To control the reflection coefficient of each unit cell, it is connected to a tunable electronic circuit. Given that the physical dimensions of the unit cell are often smaller than the wavelength of the incident wave, its behavior can be approximated using an equivalent lumped circuit model [60]. In this model, the metallic components of the unit cell are represented as inductors. Thus, the electrical characteristics of the unit cell become equivalent to a parallel resonant circuit as shown in Fig. 3.4 [61].

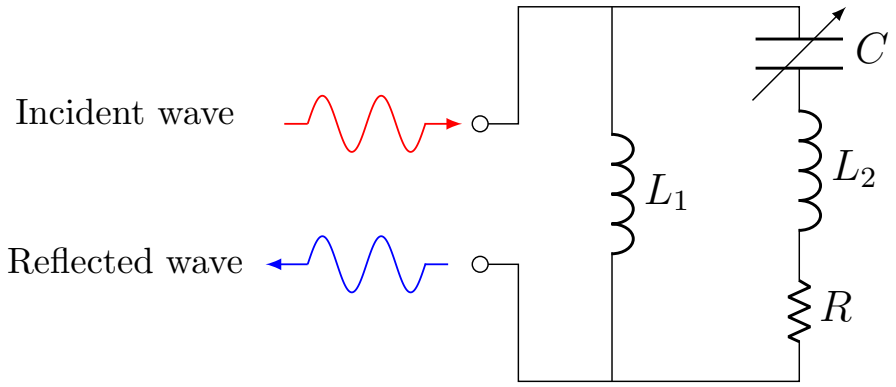

FIGURE 3.4 – Equivalent lumped circuit for a unit cell in a practical RIS

3.2 Applications of IRSs

Within this section, we will provide a concise overview of several potential applications that address inherent constraints in traditional wireless communications while introducing novel technologies through the manipulation of the radio environment. In these specific use cases, the reconfigurable intelligent surface (RIS) is customized to address particular optimization challenges based on the desired performance metrics. Consequently, these applications go beyond solely harnessing the electromagnetic capabilities of the RIS.

- Coverage enhancement : By utilizing a Reconfigurable Intelligent Surface (RIS), it becomes possible to establish simulated connections between the base station (BS) and users who experience inadequate signal strength or obstructions [62], [63], as depicted in Figure 3.5.(a). This particular application holds great potential for extending coverage, particularly in scenarios involving millimeter-wave (mmWave) and terahertz communications, which are susceptible to blockage from physical obstacles.

- Simultaneous information and wireless power transfer (SWIPT) : By leveraging its impressive beam-focusing capabilities, a Reconfigurable Intelligent Surface (RIS) directs incoming waves towards energy-demanding devices, enabling simultaneous information and power transfer [64], [65]. This particular application holds great promise in various domains, including Internet of Things (IoT) and sensor networks, offering potential solutions for enhanced functionality and efficiency.

- Physical layer security : The deliberate deployment of a Reconfigurable Intelligent Surface (RIS) aims to intentionally degrade the signals intercepted by eavesdroppers. This is accomplished by configuring the RIS to cause destructive interference between the reflected links passing through it and the signal received by the eavesdropper, thereby reducing the potential leakage of confidential information [66], [67], as illustrated in Figure 3.5.(b).

- Positioning : This particular application involves leveraging large Reconfigurable Intelligent Surfaces (RISs) to generate precise pencil-like beams in three-dimensional space, enabling accurate positioning estimation of terminals [68], [69]. It holds great promise, particularly for indoor localization scenarios where conventional global positioning systems often encounter challenges due to signal blockage affecting satellite-based positioning.

- Rank improvement : In Line-of-Sight (LoS) environments, the MIMO channel matrix often lacks full rank, making spatial multiplexing unachievable. However, by deploying distributed Reconfigurable Intelligent Surfaces (RISs) as artificial scatterers, it becomes possible to synthesize a form of multipath propagation. This approach introduces additional degrees of freedom and effectively addresses this inherent limitation [70], [71], [72], as depicted in Fig.3.5.(c).

- RIS-assisted cell edge users : By deploying a Reconfigurable Intelligent Surface (RIS) at the cell edges, it becomes possible to address the challenges faced by users who typically experience significant signal attenuation from their serving base stations (BS) as well as high interference from neighboring BSs. In this scenario, the RIS is used to ensure that the reflected signals are combined constructively at the intended users, creating a signal hot-spot. Simultaneously, the reflected signals are combined destructively at unintended users, creating an interference-free region [73], as illustrated in Fig.3.5.(d).

- RIS-assisted massive device to device (D2D) communications : In this scenario, the RIS is deployed to act as a reflection hub to serve the communications between a massive number of low power devices where the reflected signals are added constructively at the desired user and destructively at undesired users [74], [75], as shown in Fig.3.5.(e).

- RIS-assisted modulation : The RIS exhibits great potential as an access point for information transmission. In this scenario, the RIS utilizes either an ambient or dedicated RF source for information encoding. By manipulating specific characteristics of the reflected signal, such as amplitude, phase, or polarization, the RIS effectively encodes the information data [76], [77], [78], [79], as illustrated in Fig.3.5.(f).

3.3 The Challenges facing the application of IRSs

In this section, we provide a concise overview of the primary challenges that could hinder the potential benefits of RIS in wireless communications applications.

3.3.1 Channel estimation

Channel estimation poses a significant challenge in achieving performance improvements in RIS-assisted wireless communications. The process of tuning the reflection coefficients of the unit cells in the RIS relies heavily on accurate channel estimation.

In RIS applications, channel estimation is more complex compared to traditional communications, as it requires estimating not only the direct channel between the base station (BS) and the user but also the channels between the RIS and the BS, as well as the RIS and the user. Furthermore, the RIS lacks powerful signal processing capabilities, adding to the difficulty of channel estimation.

The direct channel between the BS and the user can be estimated by configuring the RIS in the absorption mode and employing conventional channel estimation techniques. However, efficient and advanced techniques are needed to estimate the RIS/BS and RIS/user channels while minimizing power consumption and complexity of the RIS.

Depending on the hardware capabilities of the RIS, various techniques can be employed to estimate the RIS/BS and RIS/user channels. When dealing with nearly passive RIS, which lacks RF chains and signal processing capabilities, performing channel estimation through transmitting, receiving, and processing training signals becomes impractical.

One approach, proposed in [80], is the cascaded channel estimation technique. This method involves activating a single element at a time while deactivating the others. By transmitting a pilot signal from the user, the product of the channels between that specific element and both the BS and the user can be estimated at the BS. However, this technique introduces a significant estimation delay due to the large number of elements typically present in the RIS. Additionally, channel estimation accuracy may suffer as only one element is activated at a time.

Another approach, presented in [81], involves beam training estimation. Instead of explicitly estimating the RIS/BS and RIS/user channels, the RIS rapidly adjusts the reflection coefficients of its elements using a predefined codebook. Based on the feedback of the received signal strength from the user, the optimal beam configuration is selected for the RIS. This technique eliminates the need for explicit channel estimation but still requires efficient beam selection algorithms.

An alternative approach, introduced in [82], incorporates active elements in the RIS connected to RF chains and baseband processing units. This enables feasible channel estimation at the RIS by utilizing training signals from the BS and users. However, this approach increases the complexity and power consumption of the RIS. Nonetheless, due to the high channel correlation between adjacent elements in the RIS, accurate estimation results can be achieved even with a limited number of active elements.

3.3.2 RIS reconfiguration

In traditional wireless communication, much research has been devoted to the optimization of transmitter and receiver configurations based on the wireless channel characteristics. However, in RIS-aided wireless communication, the propagation environment itself becomes a parameter to optimize, and the RIS consists of a large number of elements. As a result, reconfiguring the RIS in wireless applications becomes highly complex.

The problem of RIS reconfiguration typically involves multiple non-convex constraints, further increasing the complexity of the optimization problem. In existing literature, RIS reconfiguration problems are often tackled using alternating optimization techniques, but these methods can be computationally intensive and may not be feasible in real-time scenarios.

To address this challenge, there is a need for lightweight algorithms that can efficiently reconfigure the RIS in real-time, considering the multiple constraints and complexities involved. Such algorithms would enable the dynamic adjustment of the propagation environment to optimize the performance of RIS-aided wireless communication systems.

3.3.3 Network optimization

Managing a network with multiple base stations (BSs) and distributed reconfigurable intelligent surfaces (RISs) to cater to a large user population poses significant challenges in real-time configuration. The network comprises various disjointed components, making it difficult to achieve a global optimum across the entire network. Attaining such optimization would demand an extensive number of control signals for resource allocation, power allocation, user scheduling, and RIS configuration.

To address this complexity, it is vital to develop novel network optimization schemes that strike a balance between computational efficiency and energy consumption. These schemes should provide reasonable overhead while achieving the desired configuration and optimization objectives for the network, considering the involvement of multiple BSs, RISs, and a massive number of users.

3.4 A Literature Review on IRSs

The utilization of Intelligent Reflecting Surfaces (IRS) for supporting diverse applications in wireless transmission has prompted extensive research. Previous studies in the realm of IRS have encompassed a broad spectrum of subjects, including beamforming, channel estimation, resource allocation, and hardware implementation. In the course of these studies, both subjective and objective factors have been taken into account.

Subjective issues pertaining to IRS are those that can be influenced and controlled by designers. These include parameters like the power constraint of IRS, the constraint on control bits, and the quantity of IRS units, all of which can be subjectively determined.

In contrast, objective issues are beyond subjective control but are considered during the transmission design phase. These encompass factors such as the count of transceivers, the spatial gap between IRS and transceivers, and hardware impairments. These elements objectively exist in relation to the IRS configuration.

To provide a more detailed categorization, we proceed to examine the following four transmission schemes, each of which addresses distinct subjective and objective issues.

- Single IRS assisted single user (SU) transmission.
- Single IRS assisted MU transmission.
- Multiple IRSs assisted SU transmission.
- Multiple IRSs assisted MU transmission.

3.4.1 SU Transmission Based on Single IRS

A significant portion of the research on wireless transmission involving IRS has its roots in the design for Single User (SU) scenarios and scenarios involving a single Base Station (BS). In this context, Yan et al. [83] introduced an approach aimed at maximizing the received power for SU within a Multi-Input Single-Output (MISO) scheme. This was achieved by creating a passive beamforming phase shift on the IRS. Moreover, their work considered the optimization of information transfer from the IRS to the BS, which was achieved by simultaneous control of the ON-OFF states of individual elements. The study conducted in [84] focused on maximizing received power and introduced a manifold optimization technique to effectively address the constant modulus constraint. In the research presented by Perovi *et al*. [85], the analysis of Single User (SU) channel capacity involves the utilization of the global co-phasing technique. This technique is applied to devise the phase configuration of the IRS. Importantly, the study takes into account a jointly optimized scenario involving Multiple-Input Multiple-Output (MIMO) considerations.

3.4.2 MU Transmission Based on Single IRS

In systems where a single Intelligent Reflecting Surface (IRS) is utilized, managing Multiple Users (MU) becomes a more comprehensive yet intricate task. In this context, a solitary IRS can play a dual role – enhancing Quality of Service (QoS) for users in specific areas under IRS coverage, but also potentially deteriorating QoS for other users. In the study documented in [45], the semidefinite relaxation (SDR) technique was applied. This method provides a high-quality approximate solution to enhance Multi-User (MU) downlink transmission while adhering to modulus constraints.

Additionally, the incorporation of IRS into communication systems has been explored from various perspectives. These include endeavors aimed at maximizing Energy Efficiency (EE) and optimizing the weighted sum rate [86], [87].

3.4.3 SU Transmission Based on IRS Networks

The concept of an Intelligent Reflecting Surface (IRS) network, involving the deployment of multiple IRS components within a transmission environment, has been investigated to achieve enhanced Energy Efficiency (EE) and Spectral Efficiency (SE). Leveraging a supervised learning approach, the IRS network has been employed to maximize the throughput of a Single User (SU) [88].

3.4.4 MU Transmission Based on IRS Networks

Research into Multi-User (MU) transmission through an IRS network has also been conducted. This investigation takes into account the minimization of power consumption for transmit beamforming, while adhering to constraints related to power supply, Signal-to-Interference-plus-Noise Ratio (SINR) at each receiver, and maintaining a constant modulus [89]. In the study presented in [90], a statistical path loss model for an extensive Intelligent Reflecting Surface (IRS) network is formulated. This model takes into account both the user (UE) and Base Station (BS) density to calculate and determine the extent of blind-spots within the coverage area.

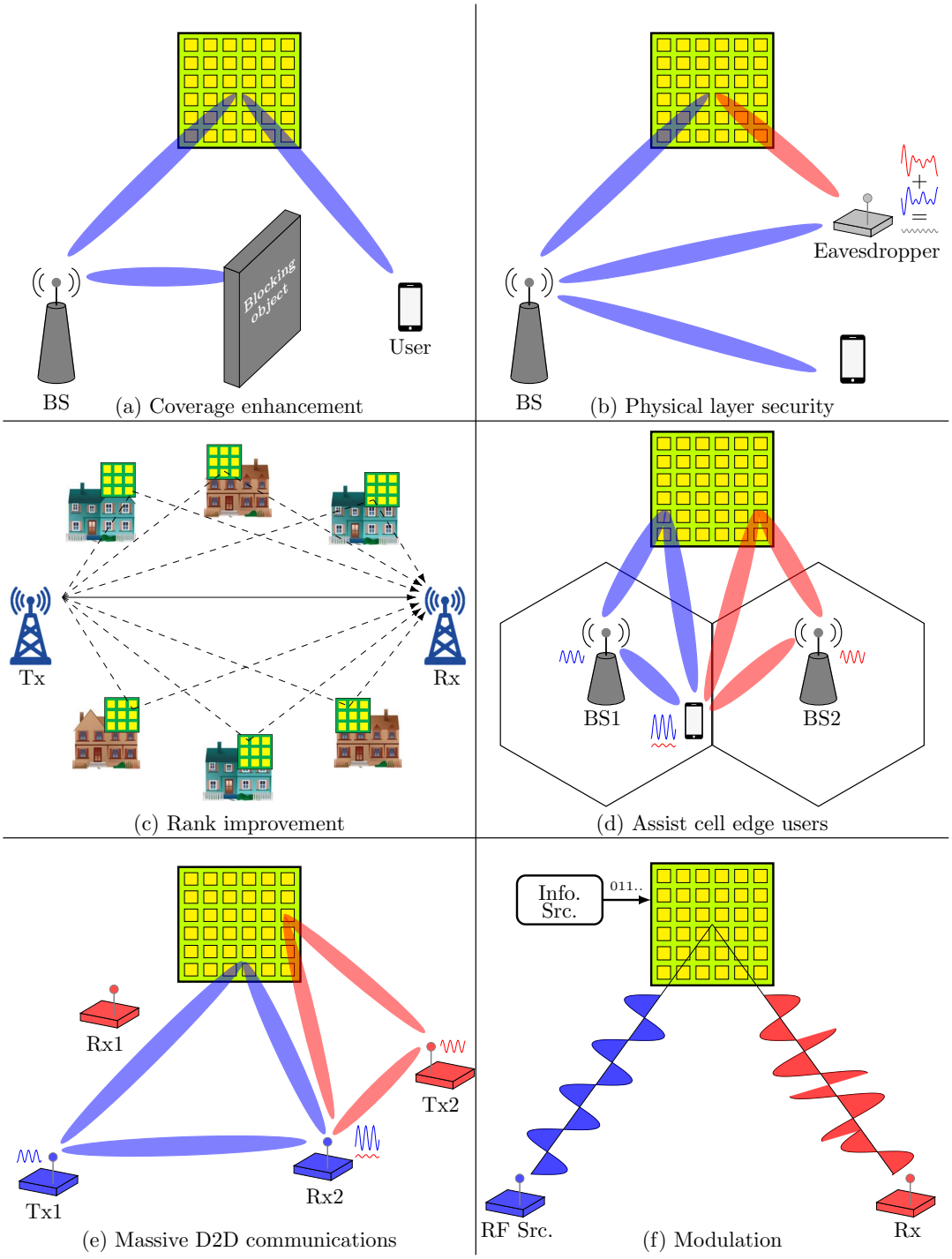

FIGURE 3.5 – Applications of IRSs

4

Wireless communications assisted by hybrid IRSs-NOMA

In this chapter, we'll go trough an introduction to IRS-aided NOMA networks. Then, we'll conduct a literature review on it. After that, we'll present its system and channel models. Finally, we'll detail its outage performance in both downlink and uplink scenarios.

4.1 Introduction

Intelligent Reflecting Surfaces (IRS) serve as a cost-efficient and energy/spectral resource-efficient solution, strategically adapting the propagation environment of mobile users to enhance reception reliability and user data rates, as highlighted in references [45] and [91].

A distinguishing aspect of an IRS compared to a half-duplex (HD) relay lies in its operational principle. While an HD relay actively processes the incident signal, an IRS functions by intelligently reflecting and beam-forming the incoming signal, thus consuming less energy. Additionally, an IRS has the capability to operate in full-duplex (FD) mode, effectively managing signal transmission and reception simultaneously, while circumventing self-interference, as mentioned in reference [91].

Operating as a multiple-access (MA) technique, non-orthogonal MA (NOMA) introduces a dynamic spectrum sharing approach among mobile users. This strategy aids in reducing access latency, enhancing Spectral Efficiency (SE), supporting increased connectivity, and promoting equitable user treatment, as outlined in reference [92]. However, this advantage comes with the trade-off of heightened receiver complexity when compared to orthogonal MA (OMA).

An organic progression was to synergize these two technologies, allowing for a smart and efficient adaptation of the propagation environment for NOMA users. This merger capitalizes on the benefits of NOMA, which facilitates shared spectrum utilization among users, as described in references [93], [94], and [95]. In existing literature, this amalgamation is often referred to as IRS-aided NOMA, IRS-assisted NOMA, or simply IRS-NOMA.

4.2 Literature on IRSs-NOMA

IRS-NOMA has garnered substantial attention from both the academic and industrial realms. For instance, to strike a balanced trade-off between maximizing the cumulative data rate and minimizing total power consumption within a downlink Multiple-Input Single-Output (MISO) IRS-NOMA network, a resourceful energy-efficient algorithm was introduced in the work documented by Fang *et al*. [93]. In reference to [94], a distinctive configuration of an IRS-NOMA network was introduced. This design entails employing Space Division Multiple Access (SDMA) for managing proximate users, whereas multiple IRS units are harnessed to cater to users at the outer cell edges. The stUEy also delved into assessing the susceptibility of this IRS-NOMA design to the influence of hardware impairments. The work presented in [95] introduces a design centered on prioritization to enhance Spectral Efficiency (SE). This design focuses on bolstering the performance of the most robust User Equipment (UE), while the remaining users derive advantages from IRS-assisted beamforming.

Furthermore, a performance evaluation was conducted in [96], drawing a comparison between NOMA and Orthogonal Multiple Access (OMA) within an IRS-assisted downlink setup. This assessment primarily revolved around the needed transmit power. To optimize the overall throughput in a downlink IRS-NOMA network, the researchers in [97] formulated a comprehensive joint optimization problem. This problem encompassed factors such as channel assignment, the decoding sequence for NOMA users, reflection coefficients, and power allocation.

The influence of both coherent and random phase shift designs on the outage performance of a downlink IRS-NOMA network was stUEied in [98].

For ensuring equitable treatment of users, the authors of [99] embarked on maximizing the Signal-to-Interference-plus-Noise Ratio (SINR) for all users. This was achieved through a combined optimization of the phase-shift matrix at the IRS and the transmit beamforming vectors at the Base Station (BS).

In the context of a downlink IRS-NOMA network, [100] examined aspects like the outage probability (OP) and the ergodic rate (ER) of users under different successive interference cancellation (SIC) conditions, taking into account both perfect and imperfect SIC scenarios. This investigation also considered a 1-bit coding scheme.

4.3 System and channel models

In what follows, we consider an IRS-aided NOMA system. As shown in Fig. , it consists of a single-antenna base station (BS) and two single-antenna user equipments (UEs), referred to as N and F. The UE labeled N is located at the center of the cell and can establish a direct communication link with the BS. On the other hand, the UE labeled F is situated at the cell edge, which presents challenges for direct communication with the BS due to factors such as long distances and obstructing objects.

The UE labeled N is located at the center of the cell and can establish a direct communication link with the BS. On the other hand, the UE labeled F is situated at the cell edge, which presents challenges for direct communication with the BS due to factors such as long distances and obstructing objects. Therefore, the UE F relies on the assistance of an IRS to establish communication with the BS.

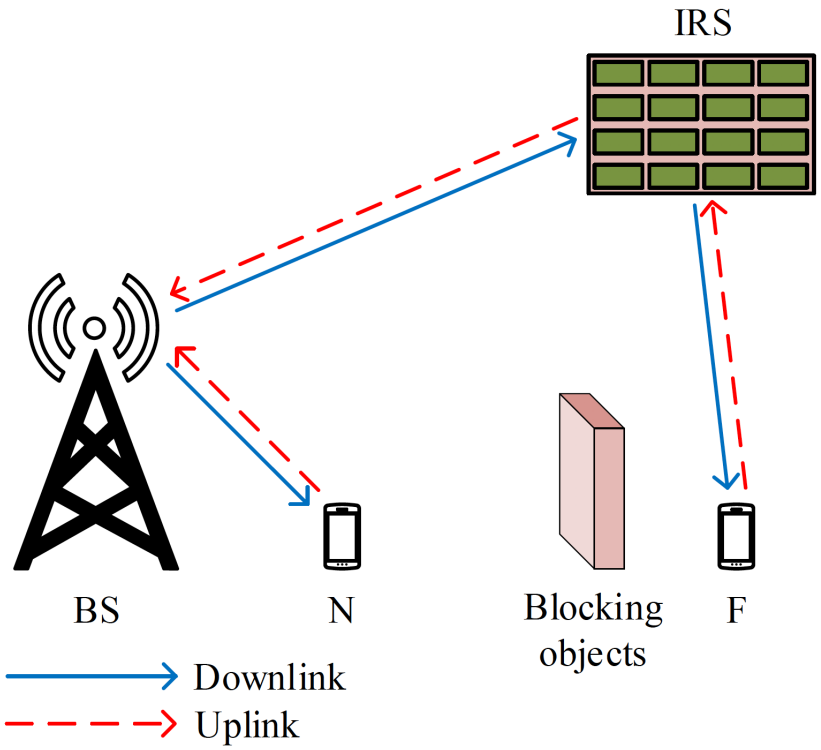

FIGURE 4.1 – The tow UEs IRS-Assisted NOMA System we have considered in this chapter [2].

The IRS has K reflective elements and its reflection coefficient matrix is denoted $\boldsymbol{\Theta} = \text{diag}\left(\zeta_1 e^{j\theta_1}, \zeta_2 e^{j\theta_2}, \ldots, \zeta_K e^{j\theta_K}\right)$, where $\zeta_k \in [0,1]$ is the amplitude reflection coefficient and $\theta_k \in [0, 2\pi)$ is the phase shift variable of the kth element which can be adjusted by the IRS $(k = 1, 2, ..., K)$[2].

Both direct and reflective channels experience quasi-static flat fading, and the CSI of all channels is assumed to be perfectly known by the BS [101] , [98]. In particular, several channel estimation schemes for IRS-assisted systems have been proposed to acquire accurate CSIs [102], [80],[103]. The link between the BS and N is assumed to be NLoS because it is a link between the BS and the UE on the ground. Therefore, the small-scale fading between BS and N follows the Rayleigh fading model and is denoted $h \sim \mathcal{CN}(0,1)$, where $\mathcal{CN}(0,1)$ is the complex Gaussian distribution. BS-IRS and IRS-F links can be LoS or NLoS for different scenarios. Due to the large path loss, signals that are reflected by the IRS twice or more are ignored. The small-scale fading vector between the BS and the IRS is denoted $\mathrm{G} \in \mathbb{C}^{1\times K}$. The small-scale fading vector between IRS and F is denoted

$\mathrm{g} \in \mathbb{C}^{K\times 1}$. In particular, these are $\mathbf{G} = [G_1, G_2, \ldots, G_K]$ and $\mathbf{g} = [g_1, g_2, \ldots, g_K]^T$, respectively. All elements of $\mathbf{G}$ and $\mathbf{g}$ follow the Nakagami-m fading pattern with fading parameters, m_G and m_g , respectively. In particular, it is NLoS for $m_{\mathcal{G}} = 1$ and is LoS for $m_{\mathcal{G}} > 1$ $(\mathcal{G} \in \{G, g\})$ [2].

For the *uplink scenario*, the signal received at the BS is given by [2]

$$y = h d_N^{-\frac{\alpha_h}{2}} \sqrt{P_u} s_1^u + \mathbf{G}\Theta g d_{F1}^{-\frac{\alpha_G}{2}} d_{F2}^{-\frac{\alpha_g}{2}} \sqrt{P_u} s_2^u + n, \tag{4.1}$$

where P_u denotes the transmit power of each UE, s_1^u and s_2^u denote signals transmitted from N and F, respectively, and n denotes the AWGN at the BS with variance σ^2. At BS, the signal from N is first decoded considering the signal from F as interference, and the corresponding SINR is given by [2]

$$\mathrm{SINR}_N^u = \frac{|h|^2 d_N^{-\alpha_h}}{|\mathbf{G}\Theta\mathbf{g}|^2 d_{F1}^{-\alpha_G} d_{F2}^{-\alpha_g} + 1/\rho'}, \tag{4.2}$$

where $\rho' = P_u/\sigma^2$ denotes the transmission SNR of each UD. After performing the SIC, the signal of F is detected with the SNR given by [2]

$$\mathrm{SNR}_F^u = |\mathrm{G}\Theta\mathrm{g}|^2 d_{F1}^{-\alpha_G} d_{F2}^{-\alpha_g} \rho' \tag{4.3}$$

When considering the *downlink scenario*, the BS transmits the signal $x = \sqrt{\alpha_1 P_b} s_1^d + \sqrt{\alpha_2 P_b} s_2^d$, where P_b denotes the transmission power of the BS, s_1^d and s_2^d denote the signals transmitted to N and F, respectively, and α_1 and α_2 represent the power allocation coefficients for N and F, respectively $(\alpha_1 + \alpha_2 = 1)$. Note that we assume that the power sharing is fixed between two UEs and that we define $\alpha_1 < \alpha_2$ for user equity. The signals received at N and F are given by [2]

$$y_N = h d_N^{-\frac{a_h}{2}} x + n_1 \tag{4.4}$$

and

$$y_F = \left(\mathrm{G}\Theta g d_{F_1}^{-\frac{\alpha_1}{2}} d_{F2}^{-\frac{\alpha_2}{2}} \right) x + n_2, \tag{4.5}$$

respectively, where d_N and d_{F1} denote the distances between the BS and N and the IRS, respectively, d_{F2} denotes the distance from the IRS to F, α_h, α_G, and α_g denotes the path loss exponents for BS-N, BS -IRS, and IRS-F links, respectively, and n_1 and n_2 denote the AWGNs at N and F, respectively, with the same variance $\sigma_{n^*}^2$.

At N, the signal of F is detected first, and the corresponding SINR is given by [2]

$$\mathrm{SINR}_{N,F}^{d} = \frac{|h|^2 d_N^{-\alpha_h} \alpha_2}{|h|^2 d_N^{-\alpha_h} \alpha_1 + 1/\rho} \tag{4.6}$$

where $\rho = P_b/\sigma_n^2$ denotes the transmission SNR of the BS. After implementation of the SIC, the signal of N is decoded, and the corresponding SNR is given by [2]

$$\mathrm{SNR}_{N}^{d} = |h|^2 d_N^{-\alpha_h} \alpha_1 \rho. \tag{4.7}$$

At F, its signal is decoded directly considering N's signal as interference, and its SINR is given by [2]

$$\mathrm{SINR}_{F}^{d} = \frac{|G\Theta g|^2 d_{F1}^{-\alpha_G} d_{F2}^{-\alpha_g} \alpha_2}{|G\Theta g|^2 d_{F1}^{-\alpha_G} d_{F2}^{-\alpha_g} \alpha_1 + 1/\rho} \tag{4.8}$$

4.3.1 Adjusting the IRS unit's parameters

The goal here is to provide the best channel quality to F by adjusting the IRS settings. That is,

$$\text{maximize } |G\Theta g| = \left| \textstyle\sum_{k=1}^{K} \beta_k G_k g_k e^{j\theta_k} \right|,$$

where G_k and g_k are the kth element of $\mathbf{G}$ and $\mathbf{g}$ respectively . This can be achieved by intelligently adjusting the phase shift variable θ_k for each element, i.e. the phases of all $G_k g_k e^{j\theta_k}$ are set to be the same. Therefore, there is not only one solution for $\{\theta_k\}$ $(k = 1, 2, \ldots, K)$, and the generalized solution is given by

$$\theta_k = \tilde{\theta} - \arg\left(G_k g_k\right),$$

where $\tilde{\theta}$ is an arbitrary constant ranging in $[0, 2\pi)$. After adopting the optimal $\{\theta_k\}$, we have [2]

$$|\mathbf{G}\Theta g|^2 = \beta^2 \left(\sum_{k=1}^{K} |G_k| \, |g_k| \right)^2 \tag{4.9}$$

where we assume that $\beta_k = \beta, \forall k$ without loss of generality.

4.4 The system's outage probability

4.4.1 Downlink scenario

For the fixed rate transmission system, outage probability is a widely used metric to measure system performance. The outage probabilities of N and F are given by [2]

$$\mathbb{P}_N^d = 1 - \mathrm{P_r}\left(\mathrm{SINR}_{N,F}^d \geq \tilde{\gamma}_F, \mathrm{SNR}_N^d \geq \tilde{\gamma}_N\right) \tag{4.10}$$

and

$$\mathbb{P}_F^d = \mathrm{P_r}\left(\mathrm{SINR}_F^d < \tilde{\gamma}_F\right), \tag{4.11}$$

respectively, where $\tilde{\gamma}_N = 2^{\tilde{R}_N} - 1$ and $\tilde{\gamma}_F = 2^{\tilde{R}_F} - 1$ with $\tilde{R}_N$ and $\tilde{R}_F$ being the target rates of N and F, respectively.

In the downlink of the IRS-assisted NOMA system under consideration, the outage probabilities of users N and F can be expressed as follows : [2]

$$\mathbb{P}_N^d = 1 - e^{-\tilde{\rho}_m} \tag{4.12}$$

and

$$\mathbb{P}_F^d \approx e^{-\frac{\lambda}{2}} \sum_{i=0}^{\infty} \frac{\lambda^i \gamma\left(i + \frac{1}{2}, \frac{\tilde{\rho}}{2}\right)}{i! 2^i \Gamma\left(i + \frac{1}{2}\right)} \tag{4.13}$$

respectively, where $\tilde{\rho}_m = \max\left\{\frac{\tilde{\gamma}_F}{(\alpha_2 - \alpha_1\tilde{\gamma}_F)a\rho}, \frac{\tilde{\gamma}_N}{a\alpha_1\rho}\right\}$ and $\tilde{\rho} = \frac{\tilde{\gamma}_F}{(\alpha_2 - \alpha_1\tilde{\gamma}_F)b\ rho}$ with $a = d_N^{-\alpha_h}$ and $b = K\beta^2(1-\xi)d_{F1}^{-\alpha_G}d_{F2}^{-\alpha_g}$. Note that when we define power allocation coefficients, we must ensure that $\alpha_2 - \alpha_1\tilde{\gamma}_F > 0$.

4.4.2 Uplink scenario

The outage probabilities of N and F are given by [2]

$$\mathbb{P}_N^u = \mathrm{P_r}\left(\mathrm{SINR}_N^u < \tilde{\gamma}_N\right), \tag{4.14}$$

and

$$\mathbb{P}_F^u = 1 - \mathrm{P_r}\left(\mathrm{SINR}_N^u \geq \tilde{\gamma}_N, \mathrm{SNR}_F^u \geq \tilde{\gamma}_F\right), \tag{4.15}$$

respectively. In the IRS-assisted NOMA system considered here, the outage probabilities of N and F for the uplink are given by [2]

$$\mathbb{P}_N^u \approx 1 - e^{-\frac{\tilde{N}_N}{a\rho'} - \frac{\lambda}{2}} \sum_{i=0}^{\infty} \frac{\lambda^i}{i! 2^{2i+\frac{1}{2}} \left(\frac{b\tilde{\gamma}_N}{a} + \frac{1}{2}\right)^{i+\frac{1}{2}}} \tag{4.16}$$

and

$$\mathbb{P}_F^u \approx 1 - e^{-\frac{\tilde{\gamma}_N}{a\rho'} - \frac{\lambda}{2}} \sum_{i=0}^{\infty} \frac{\lambda^i \Gamma\left(i + \frac{1}{2}, \frac{\tilde{\gamma}_N \tilde{\gamma}_F}{a\rho'} + \frac{\tilde{\gamma}_F}{2b\rho'}\right)}{i! 2^{2i+\frac{1}{2}} \left(\frac{b\tilde{\gamma}_N}{a} + \frac{1}{2}\right)^{i+\frac{1}{2}} \Gamma\left(i + \frac{1}{2}\right)} \tag{4.17}$$

respectively, where $\Gamma(\cdot, \cdot)$ is the upper incomplete gamma function.

5 Simulations and Results

In this chapter, we provide the simulation results for the performance evaluation of a two-user NOMA downlink network. We first illustrate the principles of successive cancellation (SC) and successive interference cancellation (SIC) through numerical examples which will be represented graphically. Then, we analyze the performance of downlink NOMA in terms of various metrics such as bit error rate (BER), achievable capacity, and outage probability. These simulations are conducted considering two different channel types : the AWGN channel and the Rayleigh fading channel. Finally, we analyze the outage probability of an uplink IRS-aided NOMA network.

5.1 Illustrating the SC and SIC functioning through numerical examples

In Section 2.3, we highlighted that superposition coding (SC) and successive interference cancellation (SIC) stand out as the two pivotal technologies enabling NOMA. In the subsequent parts of this section, we will delve into a numerical exposition of these two techniques.

Here, we consider two user equipment (UE1 and UE2) which communicate simultaneously using the same frequency with the BS. Let x_1 denote UE1's data and x_2 denote UE2's data. The principle of SC is shown in Fig.5.1.

The UE's data (x_1 and x_2) are first BPSK modulated (x_{1m} and x_{2m}) before being given different power allocations (a_1 and a_2). The superposition coded signal x_{SC} is then given by

$$x_{SC} = \sqrt{a_1}x_{1m} + \sqrt{a_2}x_{2m}, \tag{5.1}$$

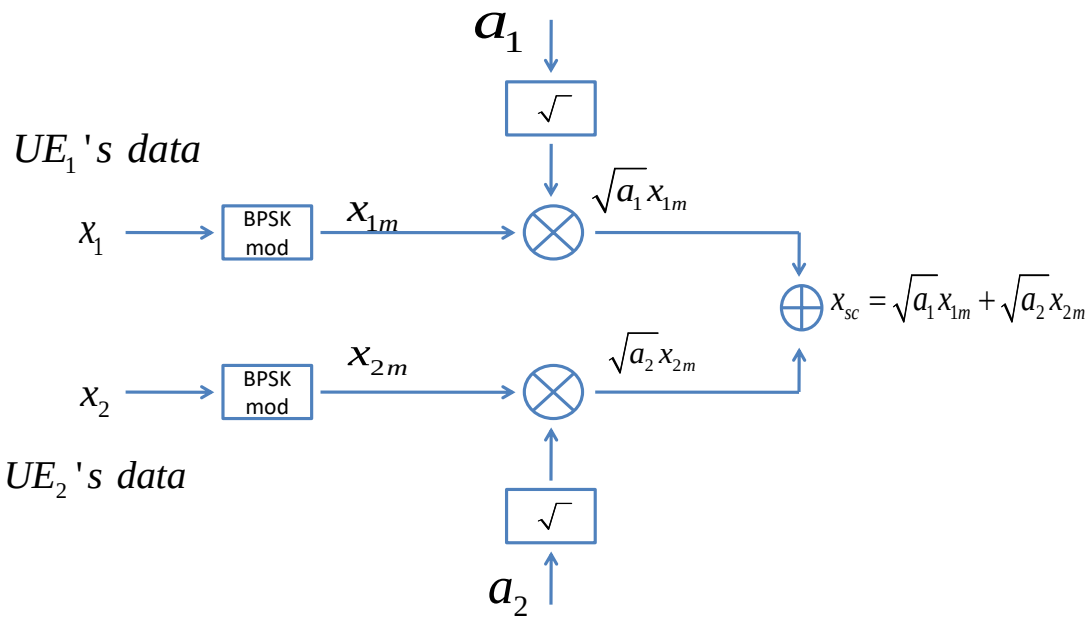

FIGURE 5.1 – The principle of SC

with $a_1 + a_2 = 1$.

As an illustrative example, let us assume that each UE has just 4 bits of data to send. This assumption is far from reality, but is sufficient to understand the basic working of NOMA. Let x_1 = 1010 and x_2= 0110. a_1=0.75 and a_2=0.25. x_1 and x_2 are graphically represented in Fig. 5.2. x_1 and x_2 must first undergo digital modulation before transmission. Let's consider BPSK modulation which maps 0's to -1's and 1's to +1's. After BPSK modulation, the mapped versions of x_1 and x_2 are shown Fig. 5.3.

We then need to scale x_1 and x_2 with $\sqrt{a_1}$ and $\sqrt{a_2}$, respectively. The result is shown in Fig. 5.4 .

Finally, the superposition coded signal x_{SC} is plotted in the Fig. 5.5 .

Newt, we will see how SIC is carried out to decode the superposition coded signal x_{SC} at the receiver side. As shown in Fig.5.6, for our simple case of a two UE NOMA network, the steps involved in SIC are described below :

1. Directly decode x_{SC} to get the signal that is weighed with high power (i.e., x_1).
2. Multiply the signal decoded in step 1 by its corresponding weight $\sqrt{a_1}$ and subtract it from x_{SC} to get $\sqrt{a_2}x_{2m}$.

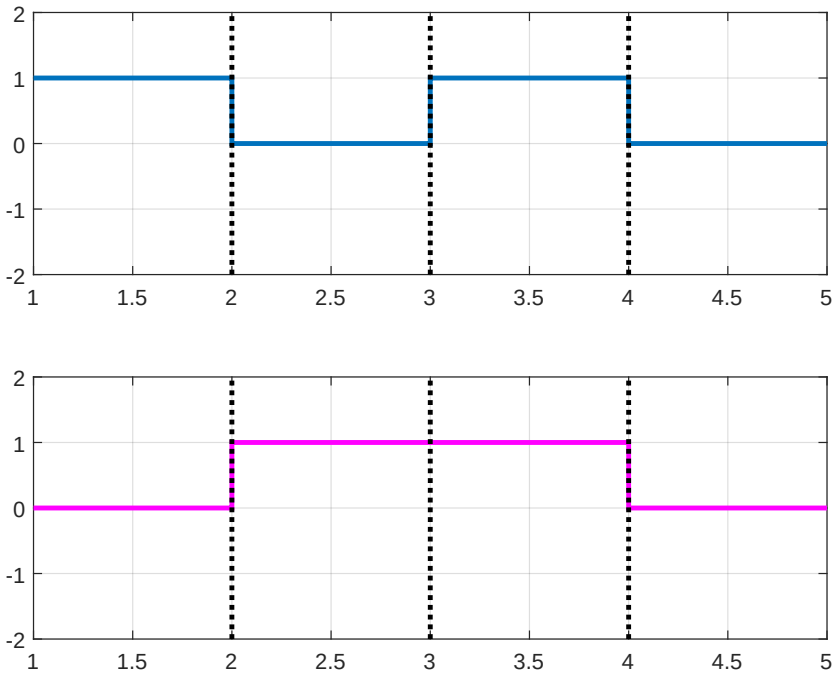

FIGURE 5.2 – Graphical representation of x_1 and x_2.

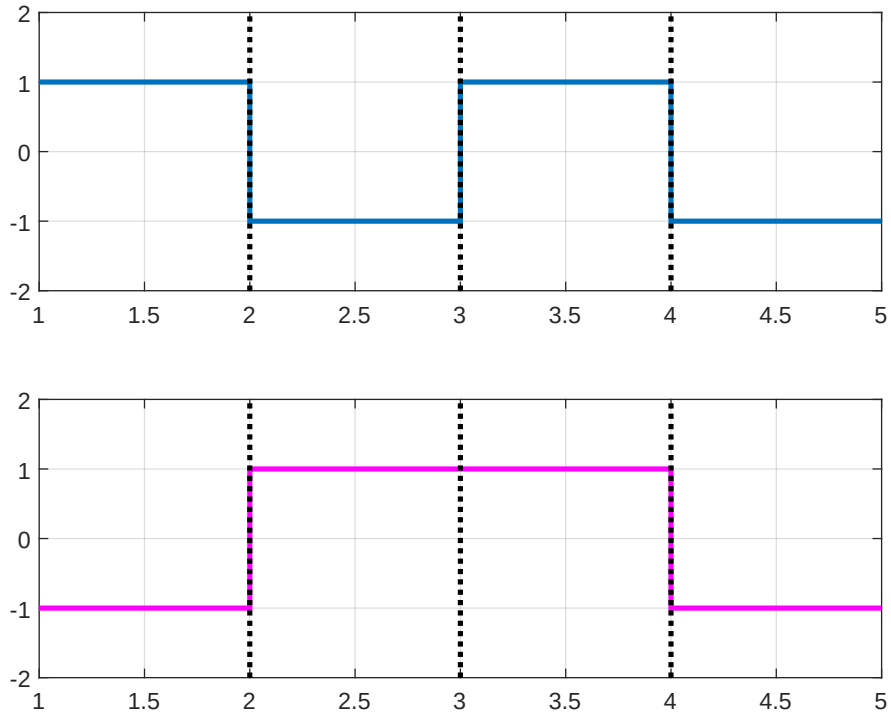

FIGURE 5.3 – x_1 and x_2 after BPSK modulation.

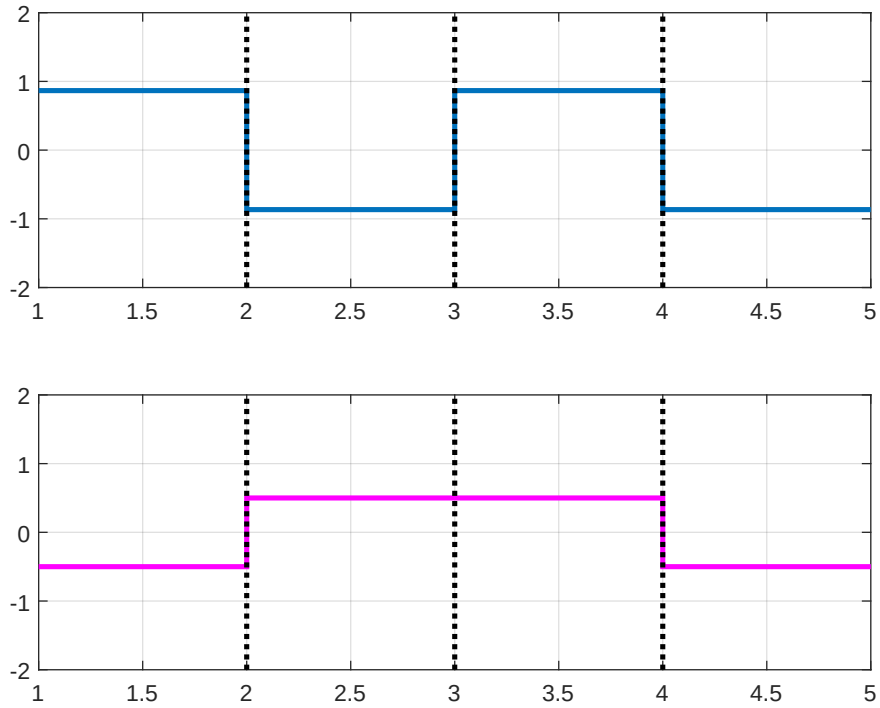

FIGURE 5.4 – Graphical representation of $\sqrt{a_1}x_1$ and $\sqrt{a_2}x_2$.

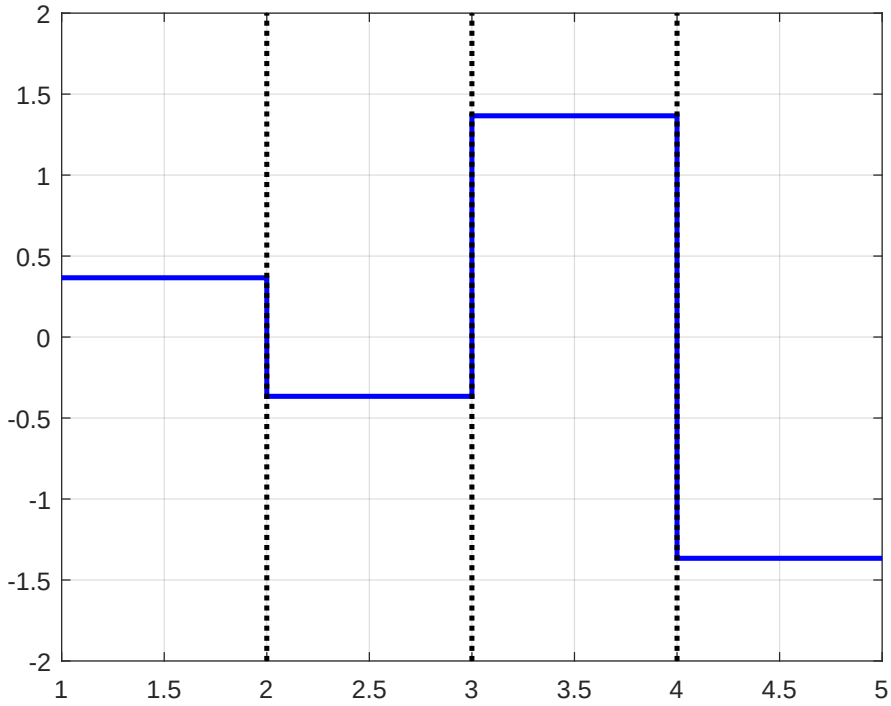

FIGURE 5.5 – The superposition coded signal x_{SC}.

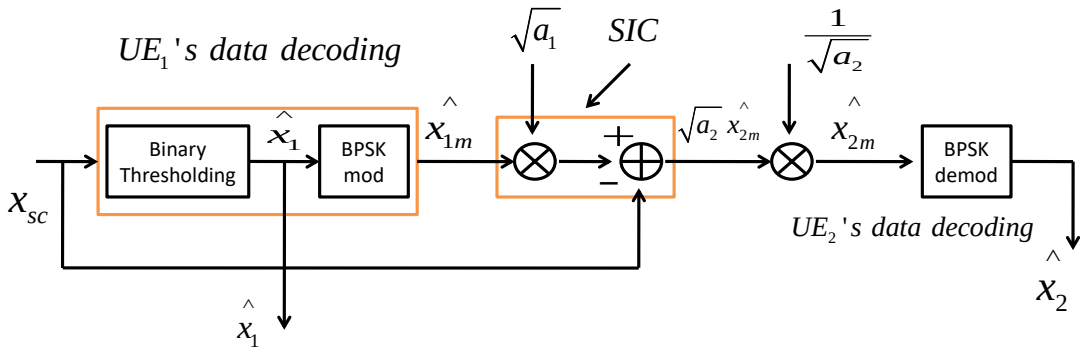

FIGURE 5.6 – The principle of SIC

3. Decode the signal obtained in step 2 to get the other signal which was multiplexed with low power (i.e.,x_2).

5.2 Downlink NOMA

5.2.1 The bit error rate (BER)

In Fig.5.7 (where the BER as a function of the SNR is plotted), we consider the downlink NOMA scenario, where the BS is transmits a superposition coded signal simultaneously to two UEs, using the same frequency carrier. The channel is a Rayleigh fading channel. UE1 is the far/weak as he is far away from the transmitting BS. UE2 is the near/strong user. Let d_1=1000 meters and d_2=500 meters, denote their distances from the BS. Let h_1 and h_2 denote the channel from the BS to the near and the far user respectively. Let's set the power allocation factors as $\alpha_1 = 0.75$ and $\alpha_2 = 0.25$. We can see that for both UEs, the BER decreases as we increase the SNR. Also, UE2 outperforms UE1 in terms of BER performance.

In Fig.5.8 , we consider the downlink NOMA scenario, where the BS is transmits a superposition coded signal simultaneously to two UEs (which are located at equal distances from the BS), using the same frequency carrier. The channel is an AWGN. We have plotted the BER as a function of the SNR. We clearly see that UE2 has slightly higher BER than UE1, especially in the low SNR regime. This is because UE2 has to do SIC. While performing SIC, UE2 must first estimate UE1's data from x_{SC}. If this estimate is wrong, then, this error will reflect in the decoding

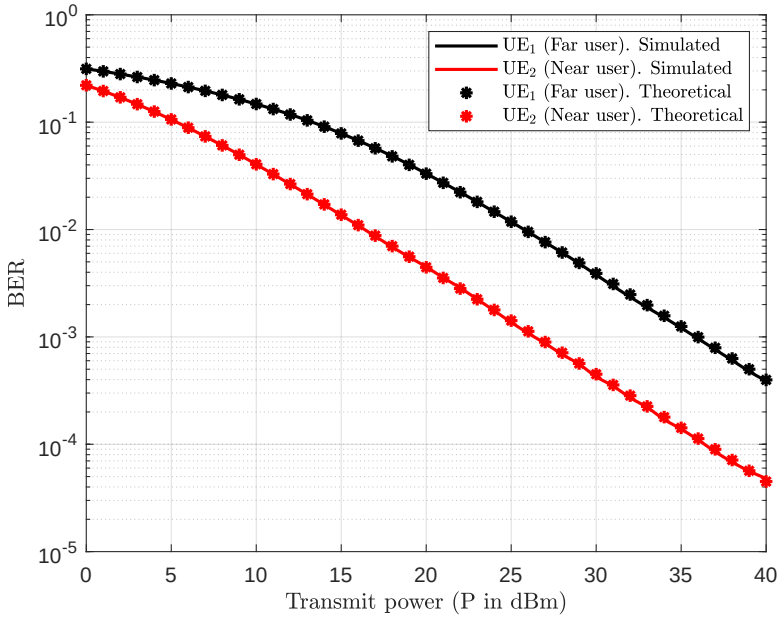

(a) $d_1 = 1000\,m, d_2 = 500\,m$

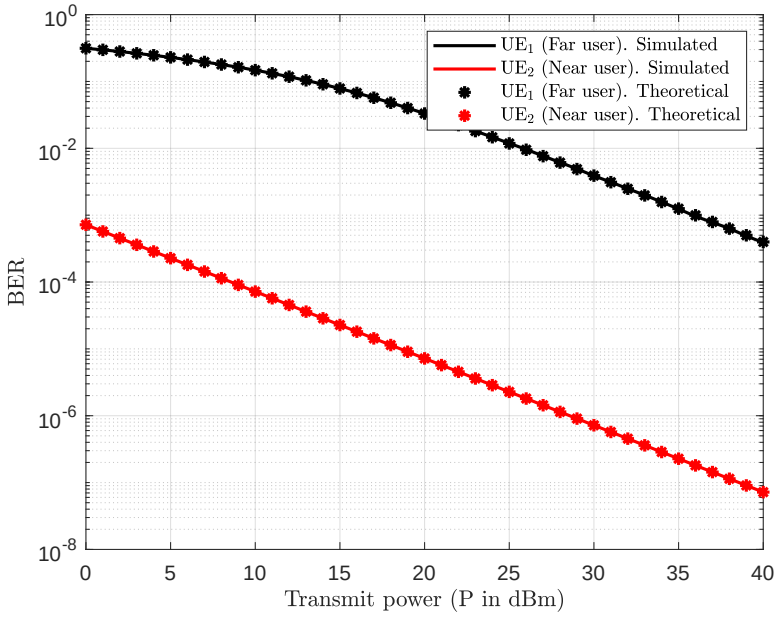

(b) $d_1 = 1000\,m, d_2 = 100\,m$

FIGURE 5.7 – The BER performance of a two UEs downlink NOMA network in a Rayleigh fading channel

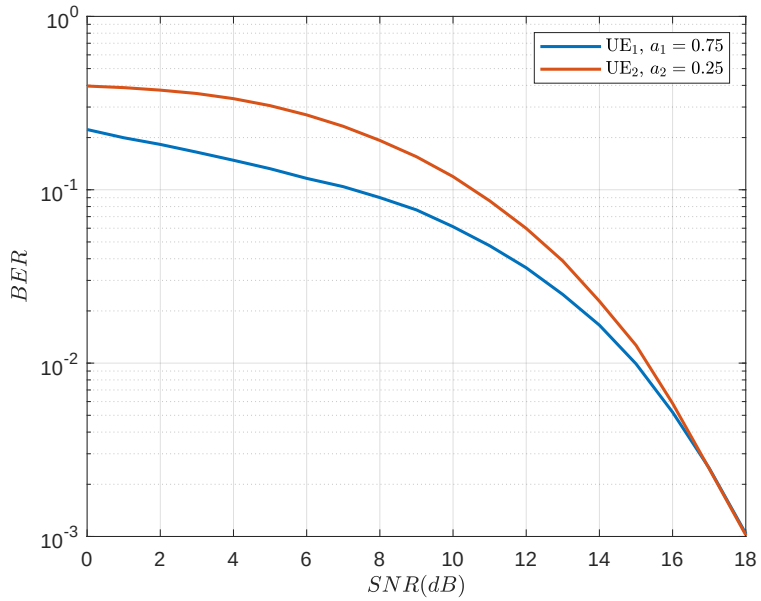

(a) $a_1 = 0.75, a_2 = 0.25$

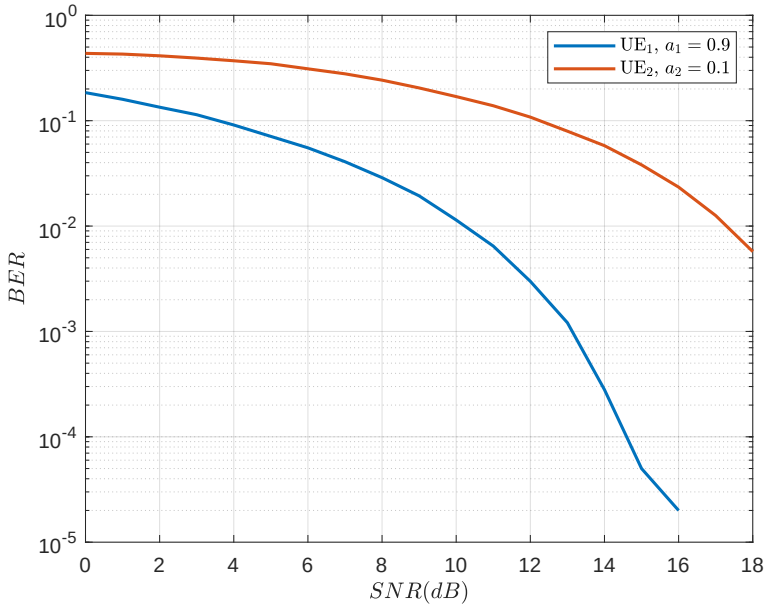

(b) $a_1 = 0.9, a_2 = 0.1$

FIGURE 5.8 – The BER performance of a two UEs downlink NOMA network in an AWGN channel.

of its own information because the wrong data would be subtracted from x_{SC}. In other words, UE2 must decode both UE1's data and its own data correctly. Any error in decoding UE1's data or its own data will impact its BER. That is why UE2 experiences higher BER than UE1.

5.2.2 The achievable capacity

Lets consider the same system model and parameters as in Fig.5.7. In Fig.5.9, we have plotted the achievable capacity of a downlink NOMA network in a Rayleigh fading channel. We can see that UE1's achievable capacity increases slowly, then stabilizes starting 30 dBm. UE2's achievable capacity increase without limit with the increase of the SNR, and it is much higher than that of UE1.

5.2.3 The outage probability

Lets consider the same system model and parameters as in Fig.5.7. In Fig.5.10, we have plotted the outage probability of a downlink NOMA network in a Rayleigh fading channel. We can clearly see that for both UEs, the OP decrease as we increase the SNR. The OP of UE2 is lower that that of UE2.

5.3 Uplink IRS-assisted NOMA

In this section, we consider a NOMA uplink with two single-antenna UEs, assisted by an N-elements IRS. At the BS (also single-antenna), the overall received signal from both the direct and reflection links is given by

$$y = \sum_{i=1}^{2} \left(\sqrt{\ell_{h_i}} h_i + \sqrt{\ell_{h_{\text{BS}}} \ell_{g_i}} \sum_{n=1}^{N} e^{j\phi_n} \mathbf{h}_{\text{BS},n} \mathbf{g}_{i,n} \right) \sqrt{P_i} x_i + w. \tag{5.2}$$

where $h_i \in \mathbb{C}$, $\mathbf{h}_{\text{BS}} \in \mathbb{C}^N$, and $\mathbf{g}_i \in \mathbb{C}^N$ are the small-scale fading coefficients of the UE-BS, BS-IRS, and UE-IRS links, respectively. $\mathbf{h}_{\text{BS},n}$ and $\mathbf{g}_{i,n}$ are the n^{th}-elements of $\mathbf{h}_{\text{BS}}$ and $\mathbf{g}_i$, respectively. The parameters ℓ_{h_i}, $\ell_{h_{BS}}$ and ℓ_{g_i} are the path-losses across the previous links. P_i and x_i are the transmit power and signal of the i^{th}-UE. w is the AWGN at the BS with zero mean and variance P_w. For all the reflective elements of the IRS, the amplitude reflection coefficient is set to 1. ϕ_n is the phase shift applied at the n^{th}-element of the IRS unit. The links are assumed to undergo a Rayleigh fading.

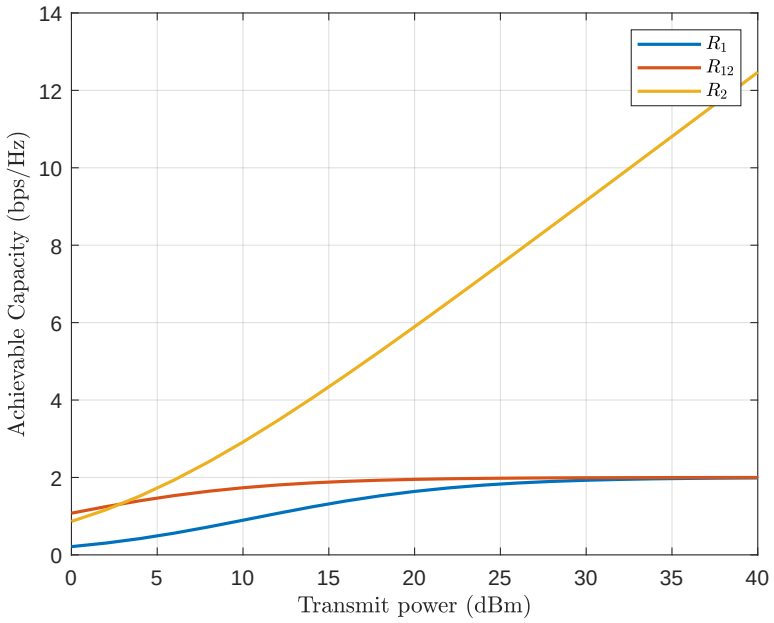

(a) $d_1 = 1000\,m, d_2 = 500\,m$

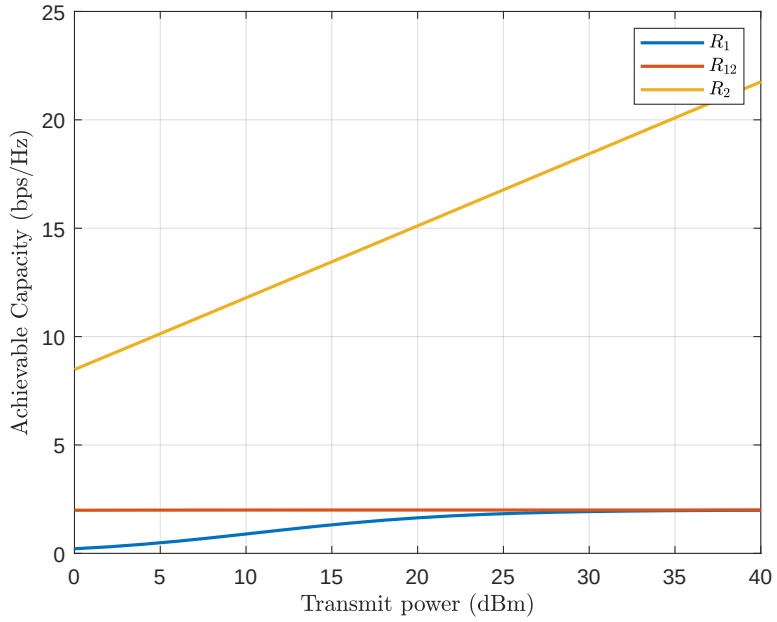

(b) $d_1 = 1000\,m, d_2 = 100\,m$

FIGURE 5.9 – The achievable capacity of a two UEs downlink NOMA network in a Rayleigh fading channel

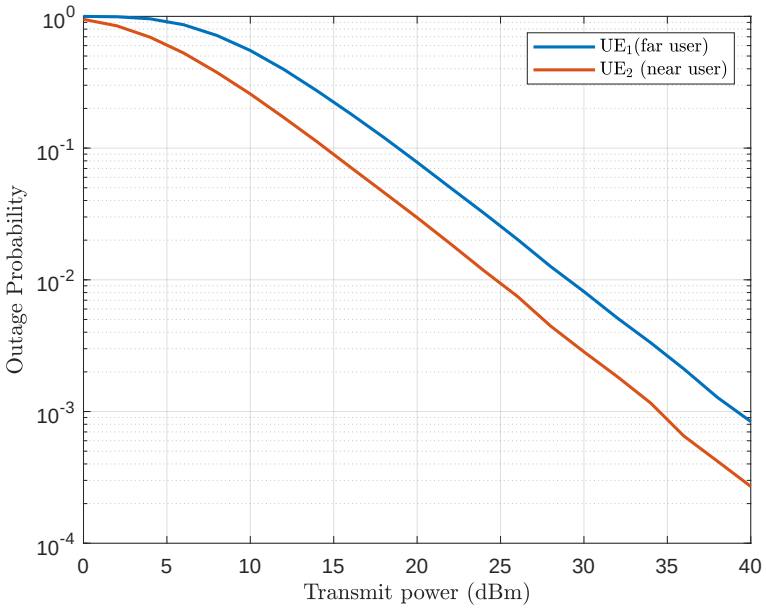

(a) $d_1 = 1000\,m, d_2 = 500\,m$

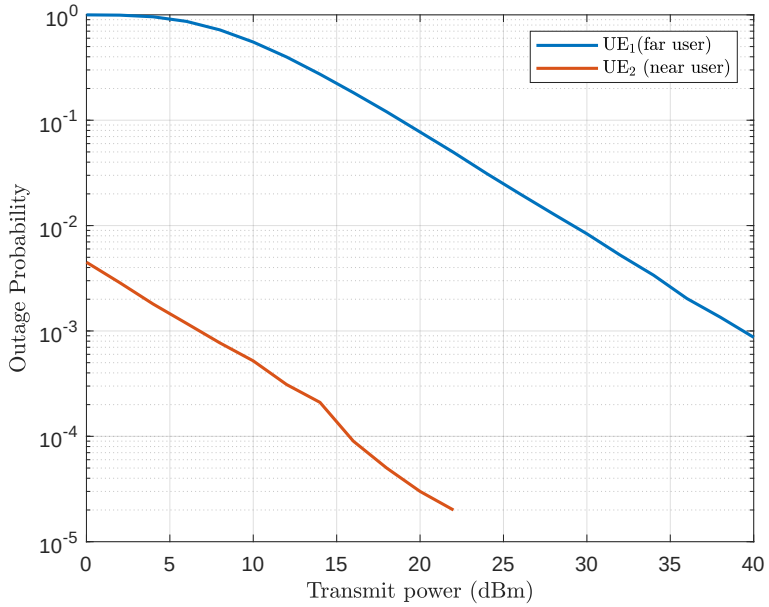

(b) $d_1 = 1000\,m, d_2 = 100\,m$

FIGURE 5.10 – The outage probability of a two UEs downlink NOMA network in a Rayleigh fading channel

Fig. 5.11 shows the OP as a function of the threshold λ_{th} for transmit powers of 20 and 30 dBm, respectively. We point out that UE_2 (which has a random phase-shifting configuration) does not benefit from the increase of the number of the IRS elements N. The reason for this is that the spatial degree of freedom offered by the IRS cannot be exploited in a random phase-shifting scheme. In the case of UE_1, the outage threshold required to achieve a given OP raises as N increases. Indeed, for a $P_{\text{out}} = 10^{-4}$, λ_{th} raises 5 dB as N increases form 16 to 128 for both values of P. Higher rates are achieved in Fig. 5.11b, where the transmit power is increased to $P = 30$ dBm.

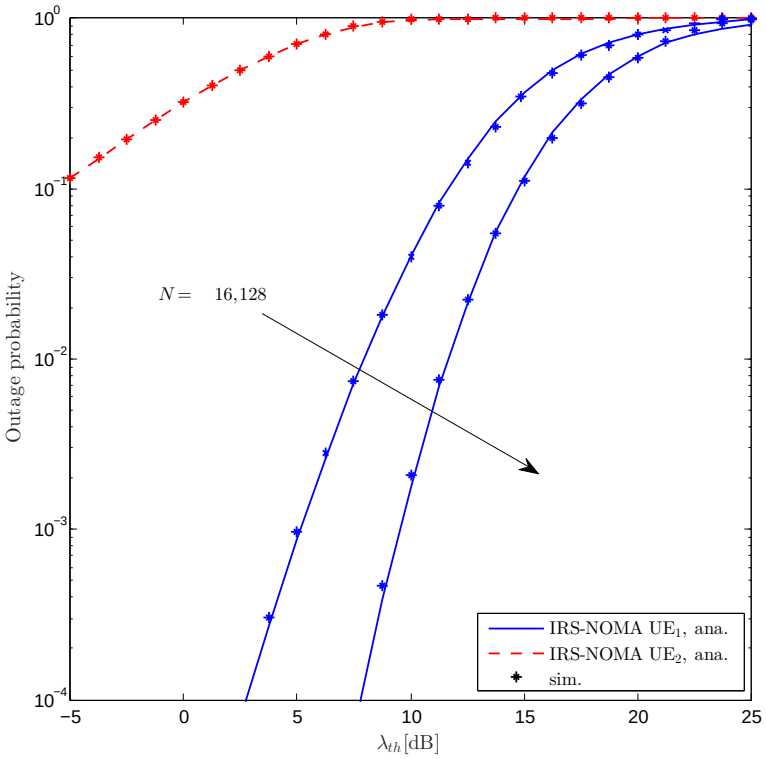

(a) $P = 20$ dBm.

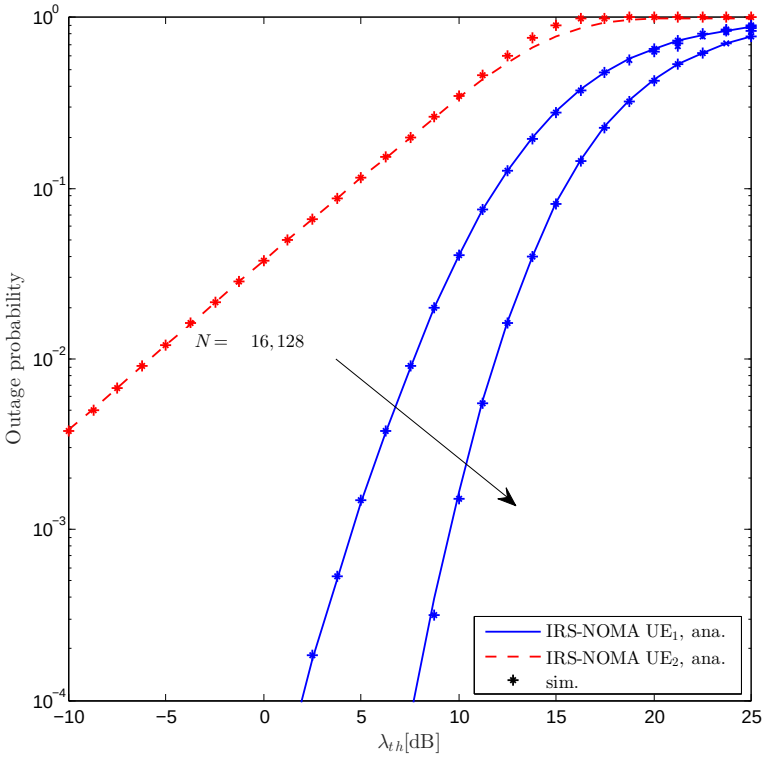

(b) $P = 30$ dBm.

FIGURE 5.11 – OP vs the outage threshold λ_{th}.

Conclusion and perspectives

In this thesis, we have carried out a study on uplink-NOMA transmission assisted by reconfigurable smart surfaces.

First, the principles of NOMA networks and IRS-assisted transmission systems were studied. The performances of NOMA and IRSs-NOMA were analyzed in terms of bit error rate (BER), achievable capacity, and outage probability.

This work highlights the power of NOMA systems assisted by IRSs.

While this thesis and other related works have made significant contributions to hybrid IRS-NOMA systems, several challenges still await resolution. Given that this work examines a single-IRS aided NOMA/OMA network, it's worthwhile to explore a multiple-IRS version wherein each User Equipment (UE) is served by a dedicated IRS. This could potentially enhance received signal quality and merits investigation in future research.

Another promising avenue is dividing the IRS unit into two segments, each catering to a UE in a coherent manner. A compelling question to answer here would be the determination of the optimal splitting ratio.

In this study, our focus has been on jointly controlling the IRS unit's parameters, especially the phase shifts, for both UEs. This was carried out by assuming perfect Channel State Information (CSI) availability at both the Base Station (BS) and the IRS unit's controller. Exploring the impact of imperfect CSI estimation on the overall system performance constitutes yet another intriguing research direction.

References

[1] Huanhuan Yang, Xiangyu Cao, Fan Yang, Jun Gao, Shenheng Xu, Maokun Li, Xibi Chen, Yi Zhao, Yuejun Zheng, and Sijia Li. A programmable metasurface with dynamic polarization, scattering and focusing control. *Scientific Reports*, 6, 2016.

[2] Yanyu Cheng, Kwok Hung Li, Yuanwei Liu, Kah Chan Teh, and H. Vincent Poor. Downlink and uplink intelligent reflecting surface aided networks : Noma and oma. *IEEE Transactions on Wireless Communications*, 20 :3988–4000, 2021.

[3] Andrea J. Goldsmith. Wireless communications. 2005.

[4] Andreas F Molisch. Wireless communications. *John Wiley and Sons*, 2012.

[5] Theodore Ted S. Rappaport. Wireless communications - principles and practice. 1996.

[6] Madan Kumar Lakshmanan and Homayoun Nikookar. A review of wavelets for digital wireless communication. *Wireless Personal Communications*, 37 :387–420, 2006.

[7] Anzar Mahmood, Nadeem Javaid, and Sohail Razzaq. A review of wireless communications for smart grid. *Renewable & Sustainable Energy Reviews*, 41 :248–260, 2015.

[8] U Cisco. Cisco annual internet report (2018–2023) white paper. *Cisco : San Jose, CA, USA*, 10(1) :1–35, 2020.

[9] Robert Pepper. Cisco visual networking index (vni) global mobile data traffic forecast update. In *Mobile World Congress*, 2013.

[10] Patrick Agyapong, Mikio Iwamura, Dirk Staehle, Wolfgang Kiess, and Anass Benjebbour. Design considerations for a 5g network architecture. *IEEE Communications Magazine*, 52 :65–75, 2014.

[11] Irina Stepanets and Grigoriy Fokin. Beamforming signal processing performance analysis for massive mimo systems. In *Next Generation Teletraffic and Wired/Wireless Advanced Networking*, 2019.

[12] Yuanwei Liu, Hong Xing, Cunhua Pan, Arumugam Nallanathan, Maged Elkashlan, and Lajos Hanzo. Multiple-antenna-assisted non-orthogonal multiple access. *IEEE Wireless Communications*, 25 :17–23, 2018.

[13] Dehuan Wan, Miaowen Wen, Fei Ji, Hua Yu, and Fangjiong Chen. Non-orthogonal multiple access for cooperative communications : Challenges, opportunities, and trends. *IEEE Wireless Communications*, 25 :109–117, 2018.

[14] Salah-Eddine Elayoubi, Sana Ben Jemaa, Zwi Altman, and Ana Galindo-Serrano. 5g ran slicing for verticals : Enablers and challenges. *IEEE Communications Magazine*, 57 :28–34, 2019.

[15] Mojtaba Vaezi, H. Vincent Poor, and Zhiguo Ding. Multiple access techniques for 5g wireless networks and beyond. 2018.

[16] Wai Man Tam, Francis Chung-Ming Lau, and Chi Kong Tse. Digital communications with chaos : Multiple access techniques and performance. 2006.

[17] Durga Prasad Malladi, Byoung-Hoon Kim, and Juan Montojo. Acquisition in frequency division multiple access systems, July 17 2012. US Patent 8,223,625.

[18] David D Falconer, Fumiyuki Adachi, and Bjorn Gudmundson. Time division multiple access methods for wireless personal communications. *IEEE Communications Magazine*, 33(1) :50–57, 1995.

[19] Tong Liu, Xiaojing Lu, and Zheng Dou. An optimal design of time division multiple access protocol for data link network. *2016 IEEE International Conference on Electronic Information and Communication Technology (ICEICT)*, pages 158–161, 2016.

[20] Jawad A. Salehi. Code division multiple-access techniques in optical fiber networks. i. fundamental principles. *IEEE Trans. Commun.*, 37 :824–833, 1989.

[21] Michele Morelli, C.-C. Jay Kuo, and Man-On Pun. Synchronization techniques for orthogonal frequency division multiple access (ofdma) : A tutorial review. *Proceedings of the IEEE*, 95 :1394–1427, 2007.

[22] S. M. Riazul Islam, Nurilla Avazov, Octavia A. Dobre, and Kyung Sup Kwak. Power-domain non-orthogonal multiple access (noma) in 5g systems : Potentials and challenges. *IEEE Communications Surveys & Tutorials*, 19 :721–742, 2016.

[23] Kun Lu, Zhanji Wu, and Xuanbo Shao. A survey of non-orthogonal multiple access for 5g. *2017 IEEE 86th Vehicular Technology Conference (VTC-Fall)*, pages 1–5, 2017.

[24] Fa-Long Luo and Charlie Jianzhong Zhang. Signal processing for 5g : algorithms and implementations. 2016.

[25] Rath Vannithamby and Shilpa Talwar. Towards 5g : Applications, requirements and candidate technologies. 2016.

[26] Anass Benjebbour, Anxin Li, Yuya Saito, Yoshihisa Kishiyama, Atsushi Harada, and Takehiro Nakamura. System-level performance of downlink noma for future lte enhancements. *2013 IEEE Globecom Workshops (GC Wkshps)*, pages 66–70, 2013.

[27] Nakamura Osamu, Goto Jungo, Hamaguchi Yasuhiro, Ibi Shinsuke, and Sampei Seiichi. Performacne comparison of superposition coding schemes for downlink non-orthogonal multiple access. 2015.

[28] SM Riazul Islam, Nurilla Avazov, Octavia A Dobre, and Kyung-Sup Kwak. Power-domain non-orthogonal multiple access (noma) in 5g systems : Potentials and challenges. *IEEE Communications Surveys & Tutorials*, 19(2) :721–742, 2016.

[29] Sergio Verdu. *Multiuser detection*. Cambridge university press, 1998.

[30] Z Tong, MS Arifianto, and CF Liau. Wireless transmission using universal software radio peripheral. In *2009 International Conference on Space Science and Communication*, pages 19–23. IEEE, 2009.

[31] Eric Blossom. Gnu radio : tools for exploring the radio frequency spectrum. *Linux journal*, 2004(122) :4, 2004.

[32] Souvik Sen, Naveen Santhapuri, Romit Roy Choudhury, and Srihari Nelakuditi. Successive interference cancellation : Carving out mac layer opportunities. *IEEE Transactions on Mobile Computing*, 12(2) :346–357, 2012.

[33] Mahmoud Aldababsa, Mesut Toka, Selahattin Gökceli, Günes Karabulut-Kurt, and Oguz Kucur. A tutorial on nonorthogonal multiple access for 5g and beyond. *Wirel. Commun. Mob. Comput.*, 2018 :9713450 :1–9713450 :24, 2018.

[34] Zhiguo Ding, Xianfu Lei, George K. Karagiannidis, Robert Schober, Jinhong Yuan, and Vijay K. Bhargava. A survey on non-orthogonal multiple access for 5g networks : Research challenges and future trends. *IEEE Journal on Selected Areas in Communications*, 35 :2181–2195, 2017.

[35] Qian Clara Li, Huaning Niu, Apostolos Papathanassiou, and Geng Wu. 5g network capacity : Key elements and technologies. *IEEE Vehicular Technology Magazine*, 9 :71–78, 2014.

[36] Jehad M. Hamamreh, Haji Muhammad Furqan, and Hüseyin Arslan. Classifications and applications of physical layer security techniques for confidentiality : A comprehensive survey. *IEEE Communications Surveys & Tutorials*, 21 :1773–1828, 2019.

[37] Yi Zhang, Huiming Wang, Qian Yang, and Zhiguo Ding. Secrecy sum rate maximization in non-orthogonal multiple access. *IEEE Communications Letters*, 20 :930–933, 2016.

[38] Yang Chen, Zhong pei Zhang, and Bingrui Li. Cooperative secure transmission in miso-noma networks. *Electronics*, 2020.

[39] Yuanwei Liu, Zhijin Qin, Maged Elkashlan, Yue Gao, and Lajos Hanzo Hanzo. Enhancing the physical layer security of non-orthogonal multiple access in large-scale networks. *IEEE Transactions on Wireless Communications*, 16 :1656–1672, 2016.

[40] Lu Lv, Fuhui Zhou, Jian Chen, and Naofal Al-Dhahir. Secure cooperative communications with an untrusted relay : A noma-inspired jamming and relaying approach. *IEEE Transactions on Information Forensics and Security*, 14 :3191–3205, 2019.

[41] Zhiguo Ding, Zhongyuan Zhao, Mugen Peng, and H. Vincent Poor. On the spectral efficiency and security enhancements of noma assisted multicast-unicast streaming. *IEEE Transactions on Communications*, 65 :3151–3163, 2016.

[42] Sean Victor Hum and Julien Perruisseau-Carrier. Reconfigurable reflectarrays and array lenses for dynamic antenna beam control : A review. *IEEE Transactions on Antennas and Propagation*, 62 :183–198, 2013.

[43] Nikolay I. Zheludev and Yuri S. Kivshar. From metamaterials to metadevices. *Nature materials*, 11 11 :917–24, 2012.

[44] Chongwen Huang, Alessio Zappone, George C. Alexandropoulos, Mérouane Debbah, and Chau Yuen. Reconfigurable intelligent surfaces for energy efficiency in wireless communication. *IEEE Transactions on Wireless Communications*, 18 :4157–4170, 2018.

[45] Qingqing Wu and Rui Zhang. Intelligent reflecting surface enhanced wireless network via joint active and passive beamforming. *IEEE Transactions on Wireless Communications*, 18 :5394–5409, 2018.

[46] Marco di Renzo, Merouane Debbah, Dinh Thuy Phan Huy, Alessio Zappone, Mohamed-Slim Alouini, Chau Yuen, Vincenzo Sciancalepore, George C. Alexandropoulos, Jakob Hoydis, Haris Gaanin, Julien de Rosny, Ahcene Bounceur, Geoffroy Lerosey, and Mathias Fink. Smart radio environments empowered by reconfigurable ai meta-surfaces : an idea whose time has come. *EURASIP Journal on Wireless Communications and Networking*, 2019 :1–20, 2019.

[47] L. F. Chen, C. K. Ong, C. P. Neo, V. V. Varadan, and Vijay K. Varadan. Microwave electronics : Measurement and materials characterization. 2004.

[48] Lei Zhang, Xiao Qing Chen, Shuo Liu, Qian Zhang, Jie Zhao, Jun Yan Dai, Guo Dong Bai, Xiang Wan, Qiang Cheng, Giuseppe Castaldi, Vincenzo Galdi, and Tie jun Cui. Space-time-coding digital metasurfaces. *Nature Communications*, 9, 2018.

[49] Tie Jun Cui, Mei Qing Qi, Xiang Wan, Jie Zhao, and Qiang Cheng. Coding metamaterials, digital metamaterials and programmable metamaterials. *Light-Science & Applications*, 3, 2014.

[50] Marco di Renzo, Alessio Zappone, Mérouane Debbah, Mohamed-Slim Alouini, Chau Yuen, Julien de Rosny, and Sergei A. Tretyakov. Smart radio environments empowered by reconfigurable intelligent surfaces : How it works, state of research, and the road ahead. *IEEE Journal on Selected Areas in Communications*, 38 :2450–2525, 2020.

[51] Bo O. Zhu, Junming Zhao, and Yijun Feng. Active impedance metasurface with full 360° reflection phase tuning. *Scientific Reports*, 3, 2013.

[52] Huanhuan Yang, Xibi Chen, Fan Yang, Shenheng Xu, Xiangyu Cao, Maokun Li, and Jun Gao. Design of resistor-loaded reflectarray elements for both amplitude and phase control. *IEEE Antennas and Wireless Propagation Letters*, 16 :1159–1162, 2017.

[53] Marek E. Bialkowski, Ashley W. Robinson, and Hyok J. Song. Design, development, and testing of x-band amplifying reflectarrays. *IEEE Transactions on Antennas and Propagation*, 50 :1065–1076, 2002.

[54] Nanfang Yu, Patrice Genevet, Mikhail A. Kats, Francesco Aieta, Jean-Philippe Tetienne, Federico Capasso, and Zeno Gaburro. Light propagation with phase discontinuities : Generalized laws of reflection and refraction. *Science*, 334 :333 – 337, 2011.

[55] Daisuke Kitayama, Yuto Hama, Kenta Goto, Kensuke Miyachi, Takeshi Motegi, and Osamu Kagaya. Transparent dynamic metasurface for a visually unaffected reconfigurable intelligent surface : controlling transmission/reflection and making a window into an rf lens. *Optics express*, 29 18 :29292–29307, 2021.

[56] Hyung Ki Kim, Dongju Lee, and Sungjoon Lim. Frequency-tunable metamaterial absorber using a varactor-loaded fishnet-like resonator. *Applied optics*, 55 15 :4113–8, 2016.

[57] Wenhao Cai, Hongyu Li, Ming Li, and Li-Yu Daisy Liu. Practical modeling and beamforming for intelligent reflecting surface aided wideband systems. *IEEE Communications Letters*, 24 :1568–1571, 2020.

[58] Hongyu Li, Wenhao Cai, Yang Liu, Ming Li, and Li-Yu Daisy Liu. Intelligent reflecting surface enhanced wideband mimo-ofdm communications : From practical model to reflection optimization. *IEEE Transactions on Communications*, 69 :4807–4820, 2021.

[59] Qingqing Wu and Rui Zhang. Towards smart and reconfigurable environment : Intelligent reflecting surface aided wireless network. *IEEE Communications Magazine*, 58 :106–112, 2020.

[60] Slawomir Koziel and Leifur Þ. Leifsson. Surrogate-based modeling and optimization. 2013.

[61] Samith Abeywickrama, Rui Zhang, Qingqing Wu, and Chau Yuen. Intelligent reflecting surface : Practical phase shift model and beamforming optimization. *IEEE Transactions on Communications*, 68 :5849–5863, 2020.

[62] Chongwen Huang, Alessio Zappone, George C. Alexandropoulos, Mérouane Debbah, and Chau Yuen. Reconfigurable intelligent surfaces for energy efficiency in wireless communication. *IEEE Transactions on Wireless Communications*, 18 :4157–4170, 2019.

[63] Qurrat-Ul-Ain Nadeem, Abla Kammoun, Anas Chaaban, Mérouane Debbah, and Mohamed-Slim Alouini. Asymptotic max-min sinr analysis of reconfigurable intelligent surface assisted miso systems. *IEEE Transactions on Wireless Communications*, 19 :7748–7764, 2020.

[64] Cunhua Pan, Hong Ren, Kezhi Wang, Maged Elkashlan, Arumugam Nallanathan, Jiangzhou Wang, and Lajos Hanzo Hanzo. Intelligent reflecting surface aided mimo broadcasting for simultaneous wireless information and power transfer. *IEEE Journal on Selected Areas in Communications*, 38 :1719–1734, 2020.

[65] Yizheng Tang, Ganggang Ma, Hailiang Xie, Jie Xu, and Xiao Han. Joint transmit and reflective beamforming design for irs-assisted multiuser miso swipt systems. *ICC 2020 - 2020 IEEE International Conference on Communications (ICC)*, pages 1–6, 2020.

[66] Xianghao Yu, Dongfang Xu, and Robert Schober. Enabling secure wireless communications via intelligent reflecting surfaces. *2019 IEEE Global Communications Conference (GLOBECOM)*, pages 1–6, 2019.

[67] Hong Shen, Wei Xu, Shulei Gong, Zhenyao He, and Chunming Zhao. Secrecy rate maximization for intelligent reflecting surface assisted multi-antenna communications. *IEEE Communications Letters*, 23 :1488–1492, 2019.

[68] Sha Hu, Fredrik Rusek, and Ove Edfors. Beyond massive mimo : The potential of positioning with large intelligent surfaces. *IEEE Transactions on Signal Processing*, 66 :1761–1774, 2018.

[69] Henk Wymeersch, Jiguang He, Benoît Denis, Antonio Clemente, and Markku J. Juntti. Radio localization and mapping with reconfigurable intelligent surfaces : Challenges, opportunities, and research directions. *IEEE Vehicular Technology Magazine*, 15 :52–61, 2020.

[70] Emad Ibrahim, Rickard Nilsson, and Jaap van de Beek. Intelligent reflecting surfaces for mimo communications in los environments. *2021 IEEE Wireless Communications and Networking Conference (WCNC)*, pages 1–6, 2021.

[71] Özgecan Özdogan, Emil Björnson, and Erik G. Larsson. Using intelligent reflecting surfaces for rank improvement in mimo communications. *ICASSP 2020 - 2020 IEEE International Conference on Acoustics, Speech and Signal Processing (ICASSP)*, pages 9160–9164, 2020.

[72] Joongsub Choi, Girim Kwon, and Hyuncheol Park. Joint beamforming design for los mimo systems with multiple intelligent reflecting surfaces. *MILCOM 2021 - 2021 IEEE Military Communications Conference (MILCOM)*, pages 267–272, 2021.

[73] Cunhua Pan, Hong Ren, Kezhi Wang, Wei Xu, Maged Elkashlan, Arumugam Nallanathan, and Lajos Hanzo Hanzo. Multicell mimo communications relying on intelligent reflecting surfaces. *IEEE Transactions on Wireless Communications*, 19 :5218–5233, 2020.

[74] Gang Yang, Yating Liao, Ying-Chang Liang, and Olav Tirkkonen. Reconfigurable intelligent surface empowered underlaying device-to-device communication. *2021 IEEE Wireless Communications and Networking Conference (WCNC)*, pages 1–6, 2021.

[75] Yashuai Cao, Tiejun Lv, Wei Ni, and Zhipeng Lin. Sum-rate maximization for multi-reconfigurable intelligent surface-assisted device-to-device communications. *IEEE Transactions on Communications*, 69 :7283–7296, 2021.

[76] Emad Ibrahim, Rickard Nilsson, and Jaap van de Beek. Binary polarization shift keying with reconfigurable intelligent surfaces. *ArXiv*, abs/2112.08172, 2022.

[77] Emad Ibrahim, Rickard Nilsson, and Jaap van de Beek. Differential polarization shift keying through reconfigurable intelligent surfaces. *ArXiv*, abs/2201.12226, 2022.

[78] Wenjing Yan, Xiaojun Yuan, and Xiaoyan Kuai. Passive beamforming and information transfer via large intelligent surface. *IEEE Wireless Communications Letters*, 9 :533–537, 2020.

[79] Ertuğrul Başar. Reconfigurable intelligent surface-based index modulation : A new beyond mimo paradigm for 6g. *IEEE Transactions on Communications*, 68 :3187–3196, 2020.

[80] Zhen-Qing He and Xiaojun Yuan. Cascaded channel estimation for large intelligent metasurface assisted massive mimo. *IEEE Wireless Communications Letters*, 9 :210–214, 2020.

[81] Boyu Ning, Zhi Chen, Wenrong Chen, Yimin Du, and Jun Fang. Terahertz multi-user massive mimo with intelligent reflecting surface : Beam training and hybrid beamforming. *IEEE Transactions on Vehicular Technology*, 70 :1376–1393, 2021.

[82] Xiaojun Yuan, Ying-Jun Zhang, Yuanming Shi, Wenjing Yan, and Hang Liu. Reconfigurable-intelligent-surface empowered wireless communications : Challenges and opportunities. *IEEE Wireless Communications*, 28 :136–143, 2021.

[83] Wenjing Yan, Xiaojun Yuan, and Xiaoyan Kuai. Passive beamforming and information transfer via large intelligent surface. *IEEE Wireless Communications Letters*, 9 :533–537, 2019.

[84] Xianghao Yu, Dongfang Xu, and Robert Schober. Miso wireless communication systems via intelligent reflecting surfaces : (invited paper). *2019 IEEE/CIC International Conference on Communications in China (ICCC)*, pages 735–740, 2019.

[85] Nemanja Stefan Perović, Marco di Renzo, and Mark F. Flanagan. Channel capacity optimization using reconfigurable intelligent surfaces in indoor mmwave environments. *ICC 2020 - 2020 IEEE International Conference on Communications (ICC)*, pages 1–7, 2019.

[86] Xie Xie, Chen He, Huixu Luan, Yang Dong, Kun Yang, Feifei Gao, and Z. Jane Wang. A joint optimization framework for irs-assisted energy self-sustainable iot networks. *IEEE Internet of Things Journal*, 9 :13767–13779, 2022.

[87] Gui Zhou, Cunhua Pan, Hong Ren, Kezhi Wang, and Arumugam Nallanathan. Intelligent reflecting surface aided multigroup multicast miso communication systems. *IEEE Transactions on Signal Processing*, 68 :3236–3251, 2019.

[88] George C. Alexandropoulos, Sumudu Samarakoon, Mehdi Bennis, and Mérouane Debbah. Phase configuration learning in wireless networks with multiple reconfigurable intelligent surfaces. *2020 IEEE Globecom Workshops (GC Wkshps*, pages 1–6, 2020.

[89] Siyuan Sun, Min Fu, Yuanming Shi, and Yong Zhou. Towards reconfigurable intelligent surfaces powered green wireless networks. *2020 IEEE Wireless Communications and Networking Conference (WCNC)*, pages 1–6, 2020.

[90] Mustafa A. Kishk and Mohamed-Slim Alouini. Exploiting randomly located blockages for large-scale deployment of intelligent surfaces. *IEEE Journal on Selected Areas in Communications*, 39 :1043–1056, 2020.

[91] Qingqing Wu and Rui Zhang. Towards smart and reconfigurable environment : Intelligent reflecting surface aided wireless network. *IEEE Communications Magazine*, 58 :106–112, 2019.

[92] Zhiguo Ding, Yuanwei Liu, Jinho Choi, Qi Sun, Maged Elkashlan, I Chih-Lin, and H. Vincent Poor. Application of non-orthogonal multiple access in lte and 5g networks. *IEEE Communications Magazine*, 55 :185–191, 2015.

[93] Fang Fang, Yanqing Xu, Quoc-Viet Pham, and Zhiguo Ding. Energy-efficient design of irs-noma networks. *IEEE Transactions on Vehicular Technology*, 69 :14088–14092, 2020.

[94] Zhiguo Ding and H. Vincent Poor. A simple design of irs-noma transmission. *IEEE Communications Letters*, 24 :1119–1123, 2019.

[95] Tianwei Hou, Yuanwei Liu, Zhengyu Song, Xin Sun, Yue Chen, and Lajos Hanzo. Reconfigurable intelligent surface aided noma networks.

[96] Beixiong Zheng, Qingqing Wu, and Rui Zhang. Intelligent reflecting surface-assisted multiple access with user pairing : Noma or oma ? *IEEE Communications Letters*, 24 :753–757, 2020.

[97] Jia kuo Zuo, Yuanwei Liu, Zhijin Qin, and Naofal Al-Dhahir. Resource allocation in intelligent reflecting surface assisted noma systems. *IEEE Transactions on Communications*, 68 :7170–7183, 2020.

[98] Zhiguo Ding, Robert Schober, and H. Vincent Poor. On the impact of phase shifting designs on irs-noma. *IEEE Wireless Communications Letters*, 9 :1596–1600, 2020.

[99] Zhiguo Ding, Lu Lv, Fang Fang, Octavia A. Dobre, George K. Karagiannidis, Naofal Al-Dhahir, Robert Schober, and H. Vincent Poor. A state-of-the-art survey on reconfigurable intelligent surface-assisted non-orthogonal multiple access networks. *Proceedings of the IEEE*, 110 :1358–1379, 2022.

[100] Xinwei Yue and Yuanwei Liu. Performance analysis of intelligent reflecting surface assisted noma networks. *IEEE Transactions on Wireless Communications*, PP :1–1, 2020.

[101] Zhiguo Ding and H. Vincent Poor. A simple design of irs-noma transmission. *IEEE Communications Letters*, 24 :1119–1123, 2020.

[102] Deepak Mishra and Håkan Johansson. Channel estimation and low-complexity beamforming design for passive intelligent surface assisted miso wireless energy transfer. *ICASSP 2019 - 2019 IEEE International Conference on Acoustics, Speech and Signal Processing (ICASSP)*, pages 4659–4663, 2019.

[103] Hang Liu, Xiaojun Yuan, and Ying-Jun Angela Zhang. Matrix-calibration-based cascaded channel estimation for reconfigurable intelligent surface assisted multiuser mimo. *IEEE Journal on Selected Areas in Communications*, 38 :2621–2636, 2020.

Abstract

The utilization of intelligent reflecting surfaces (IRSs) offers a cost-effective and energy/spectral efficient approach to enhance reception reliability and data rates for mobile users by intelligently adapting their propagation environment. Similarly, Non-orthogonal multiple-access (NOMA) is a dynamic multiple-access technique that enables efficient sharing of the available spectrum among mobile users. NOMA aids in reducing access latency, increasing spectral efficiency (SE), supporting greater connectivity, and improving user fairness.

This research focuses on the integration of these two technologies, known as IRS-aided NOMA, and investigates its performance in terms of outage probability.

Keywords : spectral/energy efficiency, 5G, OMA/NOMA, IRS-NOMA.

مُلَخَّص:

يوفر استخدام الأسطح العاكسة الذكية (IRS) نهجًا فعالًا من حيث التكلفة وفعالًا في استخدام الطاقة / الطيف لتعزيز موثوقية الاستقبال ومعدلات البيانات للمستخدمين المتنقلين من خلال تكييف بيئة الانتشار الخاصة بهم بذكاء.

وبالمثل ، فإن الوصول المتعدد غير المتعامد (NOMA) هو أسلوب ديناميكي متعدد الوصول يتيح المشاركة الفعالة للطيف المتاح بين مستخدمي الهاتف المحمول. تساعد NOMA في تقليل زمن الوصول ، وزيادة كفاءة الطيف (SE) ، ودعم اتصال أكبر ، وتحسين عدالة المستخدم.

يركز هذا البحث على تكامل هاتين التقنيتين ، والمعروفين باسم NOMA بمساعدة IRS ، ويتحقق من أدائها من حيث احتمالية الانقطاع.

Résumé

L'utilisation de surfaces réfléchissantes intelligentes (IRS) offre une approche rentable et économe en énergie/spectrale pour améliorer la fiabilité de la réception et les débits de données pour les utilisateurs mobiles en adaptant intelligemment leur environnement de propagation. De même, l'accès multiple non orthogonal (NOMA) est une technique d'accès multiple dynamique qui permet un partage efficace du spectre disponible entre les utilisateurs mobiles. NOMA aide à réduire la latence d'accès, à augmenter l'efficacité spectrale (SE), à prendre en charge une plus grande connectivité et à améliorer l'équité des utilisateurs.

Cette recherche se concentre sur l'intégration de ces deux technologies, connues sous le nom de NOMA assisté par IRS, et étudie ses performances en termes de probabilité d'outage.